

Gas turbine health assessment during start-up  
and run down using a transient model

Aron Malmberg



**LUND**  
UNIVERSITY

Thesis for the Degree of Master of Science

Thesis advisors: Professor Magnus Genrup and Anna Sjunnesson



This thesis for the degree of Master of Science in Engineering has been conducted at the Division of Thermal Power Engineering, Department of Energy Sciences, Lunds Tekniska Högskola (LTH) – Lund University (LU) and at Siemens Industrial Turbomachinery AB (SIT AB). Supervisor at SIT AB: Anna Sjunnesson; Supervisor at LU-LTH: Professor Magnus Genrup; Examiner at LU-LTH: Associate Professor Marcus Thern.

*“The world is one big data problem.”*  
-Andrew McAfee

## Abstract

**keywords:** *gas turbine, prognostics, transient operation, dynamics, modeling, Dymola, SGT-800, power generation*

Throughout the years gas turbines has been widely used for a many applications. These can be divided into mechanical drive (MD) and power generation (PG). The main difference between the two is that a gas turbine used for power generation purposes is connected to a generator instead of a mechanical load. Compared to a conventional power plant where steam has to be produced before any power is generated, the gas turbine can start and be operational within minutes. Due to this short start up time the gas turbine is often used to quickly parry variations in grid frequency. With an increased amount of wind and solar power in the energy mix there is a need for medium sized gas turbines that are able to quickly start up and be operational. However, an increased amount of starts and stops significantly reduces the expected lifespan of the components in a gas turbine. A gas turbine manufacturer depends on their ability to make correct projections of the health of their gas turbines in order to avoid break downs and unnecessary downtime. This is the reason to why many gas turbine manufacturers has developed monitoring software used for prognostic and diagnostic purposes.

Siemens has developed their own off-line monitoring system which can provide measuring data from their fleet of machines across the world with a days delay. This monitoring system has been used in conjunction with a transient computer model also developed at Siemens in order to assess the suitability of using the transient model for prognostic purposes. The start and stop process of a gas turbine has been examined since this process can provide valuable information about the health of a gas turbine since this is when the components work under the highest stress and potential faults are more easily detected.

The purpose of this thesis is to examine the start and roll out for the Siemens gas turbine SGT-800 in order to develop a monitoring method based on the comparison between the collected data and transient model. The data collection has been carried out in two stages, a manual and an automated collection. Seven data points, or time intervals, occurring during the start has been formulated and identified as relevant when monitoring the health of a gas turbine during start and stop.

The results from the manual data collection has been compared to results from the transient model in order to validate the model for monitoring use. The automated data collection has been carried out using the Siemens DMA software where the results show a promising possibility to implement the data collection method with the transient model.

## Sammanfattning

**keywords:** *gasturbin, prognostisering, diagnostik, transient drift, dynamik, modellering, Dymola, SGT-800, kraftgenerering*

Genom åren har gasturbiner använts till en mängd olika applikationer. Dessa kan i huvudsak delas in i två kategorier, mekanisk drift (MD) och kraftproduktion (PG). Den huvudsakliga skillnaden mellan de två är att en gas turbin som används för kraftproduktion är kopplad till en generator istället för en mekanisk last. Till skillnad från en konventionell kraftanläggning, där ånga måste framställas för att kunna producera elektricitet, så kan gasturbinen starta och vara redo för produktion inom loppet av minuter. På grund av detta används gasturbiner ofta för att parera variationer i elnätet med avseendet på nätfrekvensen. Med en ökad andel förnyelsebara energikällor, som sol- och vindkraft, i energimixen så finns det ett särskilt behov för mindre gasturbiner med förmåga att starta upp och producera kraft snabbt. På grund av ett ökat antal starter och stopp kommer den förväntade livslängden hos komponenterna i en gasturbin att förkortas. Gasturbintillverkaren är beroende av sin förmåga att förutse komponenternas hälsa för att undvika haveri och onödiga driftstopp. Detta är också anledningen till varför många tillverkare har lagt mycket fokus på utveckling av övervakningsmjukvara.

Siemens har utvecklat ett eget off-line övervakningssystem som ger användaren tillgång till stora mängder av data från deras flotta av maskiner över hela världen med en dags fördröjning. Detta övervakningssystem har använts tillsammans med en transient modell, också utvecklad av Siemens, för att utvärdera möjligheten av att använda den transienta modellen för övervakning. Med transient menas drift som inte är stationär. Start- och stopprocessen av en gasturbin har undersökts eftersom det är under denna fas som motorkomponenterna arbetar under högst belastning och potentiella fel kan upptäckas lättare.

Syftet med denna uppsats är att undersöka start och stop för Siemens SGT-800 gasturbin. Detta för att utveckla en övervakningsmetod som baserar sig på jämförelser mellan insamlad data och simulerad data från den transienta modellen. Datainsamlingen har utförts i två steg, ett manuellt steg och ett automatiserat. Sju datapunkter, eller tidsintervall, som inträffar under start eller stopp har utformats och identifierats som angelägna för en komplett övervakning av hälsan hos en gasturbin.

Resultatet från den manuella datainsamlingen har jämförts med simulerad data från den transienta modellen för att validera modellen för övervakning. Den automatiserade datainsamlingen har genomförts med hjälp av Siemens DMA mjukvara där resultaten visar på goda möjligheter att implementera datainsamlingsmetoden tillsammans med den transienta modellen.

## Acknowledgements

This thesis has been made possible with the input of many people, both at Siemens Industrial Turbomachinery (SITAB) and at Lund University (LU). If all were to be mentioned the list would be very long.

My biggest gratitude goes to Anna Sjunnesson, my supervisor at Siemens. With her insight into the intricate world of gas turbines she has motivated and guided me along the way during the whole project, providing valuable knowledge and understanding when silly questions were asked.

I would like to thank the department manager Lennart Näs for giving me the opportunity to be a part of the performance department, and including me in the everyday work.

I would like to offer my appreciation to the whole performance department for their help and for making me feel welcome at Siemens.

I am particularly grateful for the assistance given by Andreas Hansson, system engineer at SITAB, when patiently providing instructions to a student having software problems.

Many thanks to Prof. Magnus Genrup who first introduced me to the world of gas turbines and provided me with the opportunity to write this master thesis at SITAB. I would also like to thank Assoc. Prof. Marcus Thern, who made thermodynamics interesting and who always makes time for a conversation. My gratitude to all the employees at LU that have provided me with the knowledge to continue my professional career as a Mechanical Engineer.

Finally i would like to thank my family and loved ones for the support and motivation given to me during this project!

## Nomenclature

$\beta$	Rotor inlet air angle	[degrees/radian]
$C$	Velocity	$[\frac{m}{s}]$
$C_p$	Constant pressure specific heat	$[\frac{kJ}{(kg*K)}]$
$D$	Diameter	[m]
$H$	Total enthalpy	[kJ]
$h$	Specific enthalpy	$[\frac{kJ}{kg}]$
$m$	Mass	[kg]
$N$	Rotor speed	[rpm]
$P$	Pressure	[kPa]
$p_0$	Stagnation pressure	[kPa]
$Q$	Total heat transfer	[kJ]
$R$	Gas constant	$[\frac{kJ}{(kg*K)}]$
$S$	Total entropy	$[\frac{kJ}{K}]$
$T$	Temperature,	[K]
$W$	Total Work	[kJ]

### Abbreviations

<i>BV1</i>	Bleed valve 1
<i>BV2</i>	Bleed valve 2
<i>CBM</i>	Condition based maintenance
<i>EOH</i>	Equivalent operating hours
<i>FLC</i>	Frequency load control
<i>GPA</i>	Gas path analysis
<i>LHV</i>	Lower Heating Value
<i>RUC</i>	Run up control
<i>STC</i>	Start up control
<i>TIT</i>	Turbine inlet temperature
<i>VGW</i>	Variable guide vane
<i>VIGV</i>	Variable inlet guide vane



# Contents

<b>1</b>	<b>Introduction</b>	<b>1</b>
1.1	Background . . . . .	1
1.2	Objective . . . . .	2
1.3	Problem definition . . . . .	2
1.4	Scope . . . . .	3
1.5	Method . . . . .	3
<b>2</b>	<b>Theory</b>	<b>4</b>
2.1	The fundamentals of the gas turbine . . . . .	4
2.2	The governing laws of thermodynamics . . . . .	5
2.2.1	The first law . . . . .	5
2.2.2	The second law . . . . .	5
2.3	Steady flow energy equation . . . . .	6
2.4	Entropy . . . . .	6
2.5	Gibbs equation . . . . .	7
2.6	The Brayton cycle . . . . .	8
2.7	Dimensionless characteristic . . . . .	9
2.7.1	Surge . . . . .	12
2.7.2	Rotating stall . . . . .	13
2.8	Off-design operation . . . . .	13
2.8.1	The compatibility equation . . . . .	14
2.8.2	Impact of ambient conditions on GT performance . . . . .	14
2.9	Transient operation . . . . .	15
2.9.1	Startup procedure . . . . .	16
2.9.2	Bleed valve control . . . . .	17
2.9.3	VGV control . . . . .	17
2.10	Diagnostics, prognostics and engine monitoring . . . . .	18
2.10.1	Gas turbine condition monitoring . . . . .	18
2.11	Gas turbine performance-based monitoring . . . . .	19
2.12	Tools used . . . . .	20
<b>3</b>	<b>Methodology</b>	<b>22</b>
3.1	Literature study . . . . .	22
3.2	The SGT-800 transient model . . . . .	22
3.2.1	Fuel valve model . . . . .	23
3.2.2	Old valves . . . . .	23
3.2.3	New valves . . . . .	24
3.2.4	Bleed valve modification . . . . .	25
3.3	Data collection . . . . .	25
3.3.1	Data points . . . . .	25
3.4	Chosen sites and data collection interval . . . . .	27
3.5	Manual data collection . . . . .	28
3.6	Automated data collection and screening . . . . .	28
3.6.1	Macro working principle . . . . .	28

3.6.2	Agent development . . . . .	29
<b>4</b>	<b>Result</b>	<b>31</b>
4.1	Transient model valve update . . . . .	31
4.2	Manually collected data points . . . . .	33
4.3	Automated collection of data points . . . . .	37
<b>5</b>	<b>Analysis</b>	<b>47</b>
5.1	The valve model update . . . . .	47
5.2	The manual data collection . . . . .	47
5.3	The automated data collection . . . . .	49
5.3.1	Agent/macro development and implementation . . . . .	49
5.4	Validity of the data collection . . . . .	50
5.5	Source of error . . . . .	51
<b>6</b>	<b>Conclusion</b>	<b>53</b>
<b>7</b>	<b>Future work</b>	<b>55</b>

# 1 Introduction

For three centuries Finspångs bruk were the biggest producer of cannons, which were delivered to the Swedish and European armies. In the 16th century a Dutchman named Louis De Geer bought Finspong bruk and transformed Finspong to the center of Swedish weapon manufacturing. The production of cannons was the main focus until 1911 when the Nordiska artilleriverken went bankrupt.[1] Two years later STAL (Svenska turbinfabriks aktiebolaget Ljunström) had bought the grounds on which De Geer had produced his cannons, the deal included Finspångs slott (built 1668-1685 by Louis De Geer the younger). The production of cannons was replaced with the rather peaceful production of steam turbines. At the end of the 1950's STAL had merged with the De Laval and the company STAL-Laval was created. It was from 1962 that all of the production was concentrated to Finspong. STAL-Laval developed several successful steam turbines for maritime use, some were used in the largest ships ever produced. In 1973, during the oil crisis, many of the naval applications of STAL-Laval steam turbines were ousted. This was due to the realization that large diesels were a better choice for maritime operations because of the superior efficiency of the diesel engine during part load. The focus shifted towards steam turbines for atomic power plants, specifically for the Swedish and Finnish nuclear power plant programs. Of eighteen steam turbine strings in Sweden sixteen were delivered from Finspång.

The history of gas turbines in Finspång started in 1944 when the development of three gas turbines for jet engine use was initiated on behalf of the Swedish Air Force. Unfortunately none of the Finspång machines were chosen for the project. Because of this event focus went to the conversion of the existing aero engines into power generation units and in 1955 was the gas turbine GT35 presented. This model still exists under the name SGT-500, which is the fourth generation of the GT35, this engine produces 17 MW compared to the initial 10 MW. During the years a total of seven gas turbines has been developed in Finspong. The latest and most modern is the compact and powerful SGT-750 which is designed for both power generation and mechanical drive [1]. In 2003 Siemens acquired the company and formed Siemens Industrial Turbomachinery (SIT). The focus of SIT today is the development, service/maintenance and production of gas turbines.

## 1.1 Background

The modern day industry- and naval application of gas turbines is to produce mechanical power, this is employed to drive various loads such as compressors, pumps, generators or propellers. However the most common setting for a gas turbine is power generation (PG) when connected to a generator.[4] The introduction of volatile energy sources on the market has resulted in a need for technical solutions that keep the grid stable during a loss of renewables. A way of doing this is to use decentralized power generation in smaller scale to parry

the variations of power demand. Such challenges can be overcome with the use of gas turbines. A gas turbine has the potential to quickly achieve its maximum power output compared to traditional power plants, e.g. such as a condensation plant.

For a gas turbine a high operating temperature, combined with high rotating speeds results in an assemblage of components working close to their physical limits. Adding to the strain of the engine the need to frequently start and shutting it off, consequently leads to a shortened lifespan compared to constant steady state operation.[6] The real challenge for modern GT:s is to achieve the same level of performance, such as thermal efficiency and emission levels, that is expected from the engine during steady state operation.

Alongside the development of the gas turbine there have been an effort to develop digital aid computer programs to facilitate the analytical problems related to the GT design. This digitalization of the GT provides an invaluable tool during design, operation and maintenance and is vital for further development of the GT.[6]

Siemens has developed several computer based models to evaluate the performance of their GT models during both steady state and transient operation. During transient operation of a GT several phenomena such as surge and stall can occur. These are problematic and will be explained further in the report but signify the advantage of a correct computer model when evaluating the performance of a GT.

## 1.2 Objective

The objective of this thesis is to examine several gas turbine start ups in order to provide a basis for a new monitoring method which incorporates the transient model developed by Siemens.

This monitoring method will produce a quality factor at start up indicating specific faults and deviant behavior.

## 1.3 Problem definition

The questions to be answered in this report are:

- Can a transient model of a gas turbine be used to predict faults in a fleet of gas turbines?
- Is the collected data suitable for the prediction of deviant behavior of a gas turbine?
- Can a quality factor be created for the start?
- How should the quality factor be designed to detect faults?

## 1.4 Scope

The limitations of the project are listed below:

- This project is limited to only cover the SGT-800B1.
- The theory presented in this report will only present background information and thermodynamic equations relevant for single shaft gas turbines during start up.
- The collection of data is limited to the start up and corresponding roll out only.
- Necessary changes to the transient model is limited to the bleed and fuel valves since these will be examined further during the project.

## 1.5 Method

### 1. Literature study

A literature study will be conducted with the purpose of examine if any similar work has been done previously.

### 2. Modeling and implementation

Siemens has developed a transient model of the SGT-800, further explanation of this model will be presented in the methodology section of this report.

To be able to use the model for the purpose of this thesis some modifications have to be done. The bleed valve from the compressor along with the main and pilot valves of the fuel system will be updated.

### 3. Transient data points

A normal start up will be mapped and relevant time intervals during the start will be formulated. These time intervals will hopefully provide information about the health of the gas turbine and constitute the basis of the data collection.

### 4. Measurement acquisition and Verification

The transient data points will be collected and provide a basis for comparison to the transient model. For a data point several measurement from different sites will be collected and compared to the values provided by the transient model. This in order to create a reference value for a successful start, a quality factor.

## 2 Theory

In this chapter the reader will be introduced to the working principle of the gas turbine along with the thermodynamic equations that govern gas turbine operation. The consequences of off-design operation and transients will be explained. The methods used to monitor gas turbines will be presented together with the tools used during this project. The theory presented may also be applicable to multi shaft machines, the main focus is however limited to single shaft machines.

### 2.1 The fundamentals of the gas turbine

A simple gas turbine is comprised of three main components, the compressor, combustion chamber and the turbine as described in figure 1. The compressor is connected to the turbine through a shaft which provides the power needed for the compressor to satisfy the expected pressure ratio. The fraction of work needed by the compressor from the turbine is determined by the **back work ratio** [13]. During start up, before the turbine is able to produce any power, the compressor is driven with a starter engine.

Since the compression, combustion and expansion processes are performed in different components in a gas turbine, contrary to the process in a reciprocating engine, each component is designed individually then linked together to form a gas turbine unit. The advantage of assigning different functions to different components provides the opportunity to optimize each component for their specific task.

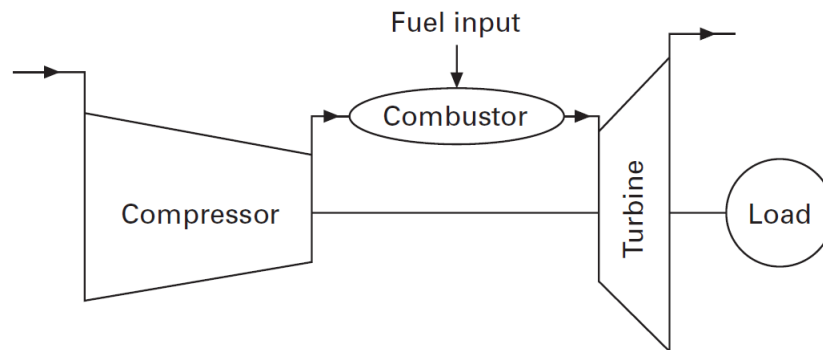


Figure 1: Schematic layout of a single-shaft gas turbine

The first step of the gas turbine cycle is the compression of the working fluid, this happens in the compressor. For the sake of comprehension imagine the compressed air being passed through the turbine assuming no losses in the process. The result would be an engine doing nothing but to turn itself over. However with the addition of energy prior to the expansion in the turbine the temperature of the working fluid can be raised. The most common way of doing

this when the working fluid is air is to inject fuel into the already hot compressed air which results in a continuous combustion. Further injection of fuel will then result in useful work.

The amount of power produced by the turbine is governed by the amount of fuel which is injected in the combustion chamber (CC). For a given amount of air mass flow there is a limited rate at which fuel can be supplied which limits the power output of the turbine. The temperature of the working fluid is increased when adding more fuel, consequently putting more strain on the highly stressed turbine blades which is limited by the creep strength and required working lifespan [8].

## 2.2 The governing laws of thermodynamics

### 2.2.1 The first law

The first law of thermodynamics states that energy cannot be destroyed only converted. For example when 50 kJ of heat is supplied to a thermodynamic system, designed to produce work, the amount of work that can be produced is up to 50 kJ [13].

### 2.2.2 The second law

The second law of thermodynamics limits the amount of work that can be produced by a device operating in a cycle, producing work from a heat source and rejecting heat to a heat sink. The process in figure 2 illustrates the working principle of a heat engine limited by the second law of thermodynamics. For example 50 kJ of heat is supplied to the engine, the amount of work that can be produced must be less than 50 kJ since the heat is also rejected to the sink, illustrated in figure 2. The ratio between the work output and supplied heat is the efficiency of the cycle. This will never be unity because if a thermodynamic process is to take place some heat will always be rejected by the system.

The maximum thermal efficiency produced by a heat engine can be expressed with equation 1 where  $T_1$  and  $T_2$  are the temperatures of the heat source and heat sink respectively. To satisfy this condition all heat addition and rejection must occur at constant temperatures ( $T_1$  and  $T_2$ ) [8].

$$\eta_{th,max} = 1 - (T_2/T_1) = \eta_{Carnot} \quad (1)$$

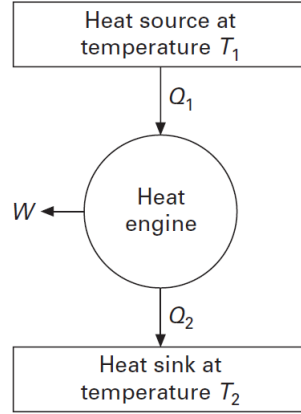


Figure 2: The working principle of the heat engine [8]

### 2.3 Steady flow energy equation

Since the energy conversion process in a gas turbine is continuous the governing equation that satisfies the first law of thermodynamics is the steady flow energy equation 2.

$$Q - W = \Delta H \quad (2)$$

$\Delta H$  can hold heat and is called the change in total enthalpy [8]. For an ideal gas the change in enthalpy can be written as:

$$\Delta H = \dot{m} \cdot C_p \cdot \Delta T \quad (3)$$

Equation 2 together with equation 3 can be expressed as:

$$Q - W = \dot{m} \cdot C_p \cdot \Delta T \quad (4)$$

### 2.4 Entropy

A way of evaluating the accessibility and availability of energy is by quantifying it with the concept of entropy. Entropy can be considered a measure of loss, where an accessible source of energy has a lower entropy value. Consequently the less available energy the higher the entropy, and the change in entropy during a process is defined as in equation 5.

$$\Delta S = \int \frac{dQ}{T} \quad (5)$$

Assume from figure 2 that the work done by the system is zero. The heat supplied would equal the total change of energy of the system and consequently the heat rejected, expressed in equation 6 [8].



$$Q = \Delta H \Rightarrow Q_1 = \Delta H = Q_2 \quad (6)$$

The total change in entropy of the system can then be expressed as in equation 7.

$$\Delta S_{system} = \Delta S_{source} + \Delta S_{sink} \Rightarrow \Delta S_{system} = \frac{Q}{T_2} - \frac{Q}{T_1} = Q\left(\frac{1}{T_2} - \frac{1}{T_1}\right) \quad (7)$$

For heat to flow from the heat source to the sink the temperature  $T_1$  must be higher than  $T_2$  and consequently equation 7 must be positive. The second law of thermodynamics states that the temperature at which heat is added and rejected must be constant. When the entropy of the source decreases the entropy of the sink will increase at a greater rate. Thus leaving the system with a positive change in entropy. This entropy change or degradation of energy is the reason why the heat rejected to the sink never can reach zero. Consequently excluding the possibility of achieving a thermal efficiency of 100 %. This condition is a direct extension from the statement of the second law of thermodynamics [8].

## 2.5 Gibbs equation

The  $\frac{dQ}{T}$  part of equation 5 corresponds to a differential change in entropy. This means that the entropy change for a process can be calculated by integrating  $\frac{dQ}{T}$  between two end states. For isothermal internally reversible processes this is of little effort. However, if the temperature varies during the two states of interest a relation between  $dQ$  and  $T$  is necessary. In this section such a relation will be presented [13].

Assuming an internally reversible process, the conservation of energy equation for a closed system can be written as:

$$\delta Q_{int rev} - \delta W_{int rev, out} = \delta U \quad (8)$$

From equation 5:

$$\delta Q_{int rev} = T ds \quad (9)$$

Boundary work:

$$\delta W_{int rev, out} = P dv \quad (10)$$

Equation 8 together with equation 9 and 10 yields the first Tds equation:

$$T dS = dU + P dV \quad (kJ) \quad (11)$$

Or:

$$T ds = du + P dv \quad (kJ/kg) \quad (12)$$

The definition of enthalpy:

$$h = u + Pv \Rightarrow dh = du + P dv + v dP \quad (13)$$

Together with equation 12 and the definition of enthalpy the second Tds equation is produced:

$$T ds = dh - v dP \Rightarrow ds = \frac{dh}{T} - \frac{v dP}{T} \quad (14)$$

## 2.6 The Brayton cycle

The operation cycle for a simple gas turbine is the Brayton cycle, it was proposed in the 1870 by George Brayton to be used in a reciprocating engine using oil for fuel [13]. It is now used for gas turbines where the compression and expansion takes place in rotating machinery. In the Ts-diagram in figure 3 the four internally reversible processes of the Brayton cycle are illustrated.

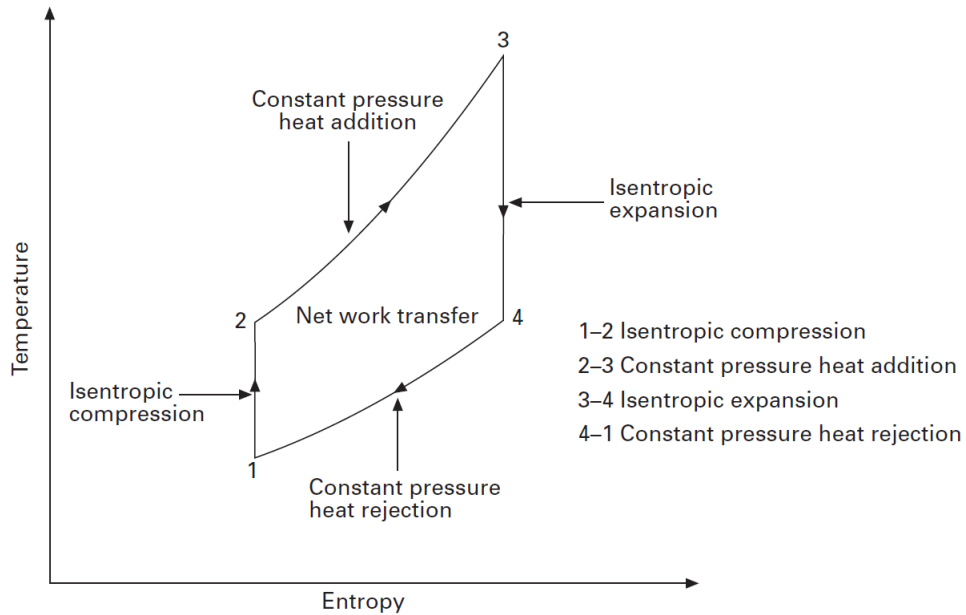


Figure 3: T-s diagram of an ideal Brayton cycle [13]

The gas turbine can be modeled as an open-cycle or closed-cycle engine. The difference being that the working fluid of the closed-cycle is constantly reused and the heat rejection and addition takes place in a heat exchanger. For the open-cycle engine, which is the more common setup, fresh air at ambient conditions is introduced into the compressor and after the expansion process in the turbine the exhaust gases is discharged to the surroundings. Therefore an open cycle would not include the constant pressure heat rejection process that occurs during process 4-1 in figure 3 [13].

For the ideal Brayton cycle the relevant steady flow energy equation can be written as in equation 15.

$$Q = (h_2 - h_1) + \frac{1}{2}(C_2^2 - C_1^2) + W \quad (15)$$

$Q$  and  $W$  are the heat and work transfers per unit mass flow. Assuming that the change of kinetic energy of the working fluid between the inlet and outlet is

negligible. Each component of equation 15 can be written as follows:

$$W_{12} = -(h_2 - h_1) = -c_p(T_2 - T_1) \quad (16)$$

$$Q_{23} = -(h_3 - h_2) = -c_p(T_3 - T_2) \quad (17)$$

$$W_{34} = -(h_3 - h_4) = -c_p(T_3 - T_4) \quad (18)$$

The cycle efficiency is defined as:

$$\eta = \frac{\text{net work output}}{\text{heat supplied}} = \frac{c_p(T_3 - T_4) - c_p(T_2 - T_1)}{c_p(T_3 - T_2)} \quad (19)$$

## 2.7 Dimensionless characteristic

The general behavior of a GT is best described using dimensional analysis. This is a procedure where a group of variables representing some physical quantity is reduced to dimensionless groups, which can be plotted against each other to present the characteristics of rotating turbo machinery. When dealing with GT performance calculation the use of dimensional analysis is a valuable tool. The performance of the compressor may be expressed using the delivery pressure, -temperature and the mass flow for a fixed value of the rotational speed. However, all of these variables depend on quantities such as the condition of the compressor entry temperature and pressure along with the properties of the working fluid. When conducting a calculation of the compressor performance the comprehension of the result is of importance. Allowing for full variation of these aforementioned variables makes a comprehensible presentation of the result is almost impossible. It is therefore common practice to employ the use of dimensionless groups when the number of variables are not to great, e.g. in GT calculation. From this method the variables involved can be combined to form more manageable dimensionless groups and also be employed to present the compressor characteristic graphically [3].

Other important applications of the dimensional analysis is the possibility to predict a turbo machines performance with test conducted on a scale model and the determination of the most suitable machine in regard to the maximum efficiency for a specific rotational speed and flow rate.[10] From the principle of dimensional analysis, also known as the Buckingham pi theorem, it is known that an equation containing M independent variables and N dimensions there must be at least M-N nondimensional groups. Consider equation 20 where seven independent variables and the three dimensions mass, length, time are present, following the pi theorem the number of nondimensional groups would then be  $7-3 = 4$ .

$$F(D, N, m, p_{01}, p_{02}, RT_{01}, RT_{02}) = 0 \quad (20)$$

For convenience the gas constant R is associated with the temperature (RT) so that the combined variable have the same dimension as velocity squared.

The gas constant can be eliminated from the final expression if the same gas have been employed in both the testing and subsequent use of the compressor. However, if any other gas is to be used in the compressor the gas constant must remain in the expression.

The presence of viscosity as a variable would result in a type of Reynolds number which in highly turbulent cases, which prevail in gas turbines, would have little or no influence over the operation range. It is therefore customary to exclude the viscosity during turbo machinery analysis. To find the problem solution equation 20 is then equated to zero.

The variables in equation 20 can now be used form the non-dimensional groups. To do this various techniques exist but generally it is of little difficulty to derive them and therefore this procedure will be omitted in this report. From equation 20 following groups can be derived:

$$\frac{p_{01}}{p_{02}} \cdot \frac{T_{02}}{T_{01}}, \frac{m\sqrt{(RT_{01})}}{D^2 p_{01}}, \frac{ND}{\sqrt{RT_{01}}} \quad (21)$$

Following the previous statement these groups can now be expressed as a function where the performance can be calculated considering the variations of delivery pressure and temperature with mass flow. When conducting analysis on a machine with a fixed diameter that compresses a known gas the variables R and D may be omitted from the equation 22.

$$F\left(\frac{p_{01}}{p_{02}} \cdot \frac{T_{02}}{T_{01}}, \frac{m\sqrt{(T_{01})}}{p_{01}}, \frac{N}{\sqrt{T_{01}}}\right) = 0 \quad (22)$$

Where  $\frac{m\sqrt{(T_{01})}}{p_{01}}$  and  $\frac{N}{\sqrt{T_{01}}}$  are named the nondimensional mass flow and rotational speed even though they truly are not dimensionless. The variations of these groups can now be plotted against one another to present the specific characteristic for a compressor. Experience has shown that the most useful way to present the characteristic is by plotting pressure- or temperature ratio against mass flow with the rotational speed as a parameters seen in figure 4 [3].

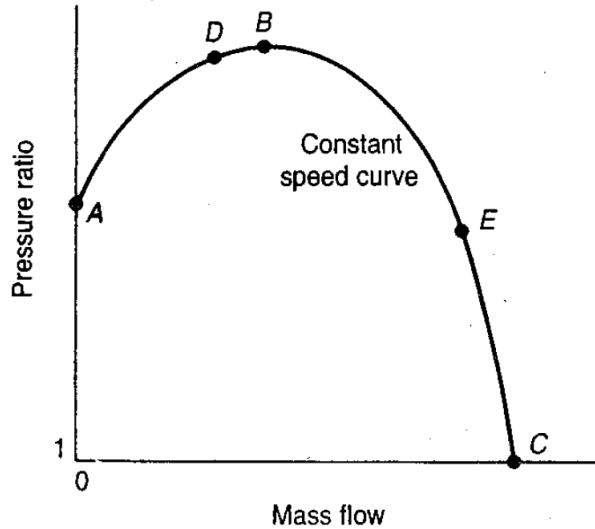


Figure 4: Theoretical characteristic of a compressor showing surge and stable operation regions [3].

The easiest way of understanding the behavior figure 4 represents is to imagine the delivery mass flow from the compressor restricted by a valve which is slowly opened. The compressor runs at a constant speed and at some point A the mass flow is zero but the pressure ratio will have some value. Opening the valve results in an increased flow through the compressor and an increased efficiency due to the pressure contribution from the diffuser vanes. At max efficiency, point B, the pressure ratio reaches its maximum. Opening the valve further, allowing for a higher mass flow results in a decrease in efficiency. This is due to the difference in angle at which the air approaches the vane which will increase. A breakaway of air will occur consequently affecting the efficiency and the pressure ratio is reduced to a point C.[3]

For a constant rotational speed the mass flow has reached some point E i figure 4 where further increase of the mass flow cannot be obtained and choking is said to have occurred. This represents the maximum mass flow for a specific rotational speed. Graphs such as the one in figure 4 may be obtained for different rotational speeds. These can be joined together so that the variation of pressure ratio is presented for the whole operating range in regard to mass flow and rotational speed, as in figure 5. The surge line represents the cumulated operating points from figure 4 where surge is initiated [3]. This is further explained in section 2.7.1. The isentropic efficiency may be plotted as contour lines superimposed on figure 5.

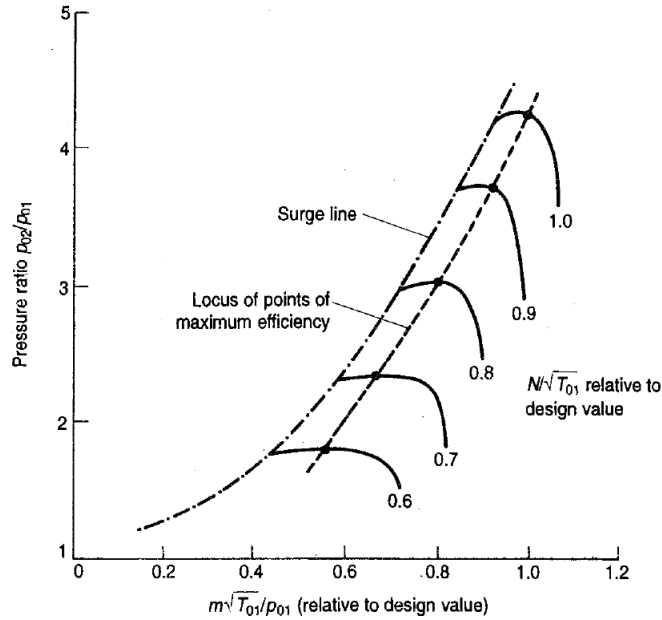


Figure 5: Compressor characteristic [3]

### 2.7.1 Surge

In figure 4 the line between point A and B cannot be obtained. This is due to the phenomenon of surge.

For GT operation a compressor that experience surge during operation is highly undesirable. During surge violent aerodynamic vibrations is transmitted throughout the whole machine and may be related to a sudden drop in delivery pressure. Imagine a compressor operating at point D in figure 4. The positive incline of the slope at point D means that a drop in mass flow would result in a drop in pressure ratio. If the pressure downstream of the compressor is not reduced quickly enough the flow of air can reverse and start flowing "upstream". The effect of this is a rapid decrease in pressure downstream since the flow has reversed to the direction of the resulting pressure gradient. A low pressure downstream allows the compressor to start the cycle over again and this can happen at a high frequency [3].

To avoid surge during operation the operating point must be located on the graph in figure 4 where the incline of the slope is negative. This would mean that for a reduction in mass flow the delivery pressure ratio would increase eliminating the possibility of a reversed flow and resulting in stable operation.

The reasons for surge to be initiated is not limited to what is mentioned here but can also depend on the swallowing capacity of other components downstream or the occurrence of rotating stall. [3].

### 2.7.2 Rotating stall

Bad performance and operational instability may be attributed to rotating stall, this occurs in the stable range (between B-C in figure 4 and can initiate surge. Rotating stall is caused by a non uniform flow approaching the blade with an increased angle of incidence. As the incidence increases the flow separates from the suction side and stalls. This leads to an increased boundary layer growth and a decreased flow area for one passage [3].

Consider figure 6. If the flow in channel B is stalled, the flow in channel A and C will increase since the flow from channel B sips over. The rotor inlet angle ( $\beta$ ), of channel A will increase while at the same time the  $\beta$  of channel C will decrease. This in turn will force the flow in channel A to separate and stall due to the increased incidence. This process will continue and rotate in the direction opposite to that of the blades. Axial compressors can operate with many of their stages stalled but rotational stall is still a reason for concern since vibrations are induced and the risk of surge is increased [8].

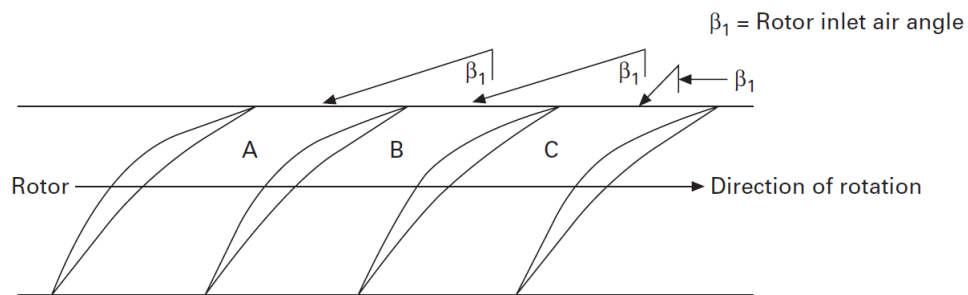


Figure 6: Rotating stall

### 2.8 Off-design operation

When designing a gas turbine the design process is usually to decide the pressure ratio, component efficiencies and the maximum cycle temperature (TIT) for an engine to achieve the desired performance. When these parameters are set the thermal efficiency and the airflow for a given power demand can be calculated. It is common for a GT to operate outside of its design point for longer periods of time and this is considered off-design operation. The reasons for off-design operation is generally a change in ambient temperature, e.g. temperature difference between winter and summer, or a change in engine load. Running a GT on part load or during a cold winter will have a significant impact on the performance. This in turn depends on the interaction of the GT components which is matched during the design process, known as component matching. This is an important step during the design process because even though a component may display a wide operating range by itself. When combined with other components, as in a GT, the component interaction can inhibit the operating range of the GT as a whole if not matched properly. [8].

### 2.8.1 The compatibility equation

To analyze the off-design performance of a GT requires several tedious calculations. The flow, work and speed compatibility equations provides a simplified analysis accurate enough to estimate the off-design performance.

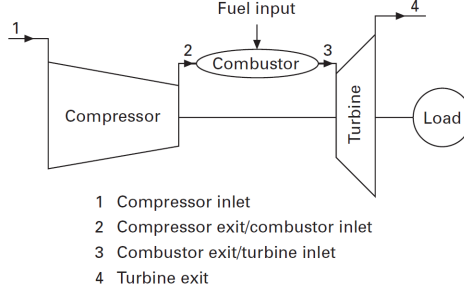


Figure 7: Schematic representation of a single-shaft GT [8]

Consider the index numbers used in figure 7, where the compressor and turbine are linked together. The compatibility of rotational speed dictates:

$$\frac{N}{\sqrt{T_3}} = \frac{N}{\sqrt{T_1}} \cdot \sqrt{\frac{T_1}{T_3}} \quad (23)$$

The compatibility of flow between the compressor and turbine can be expressed using the nondimensional groups derived earlier.

$$\frac{m_3 \sqrt{T_3}}{p_3} = \frac{m_3 \sqrt{T_3}}{p_3} \cdot \frac{p_1}{p_1} \cdot \frac{p_2}{p_2} \cdot \sqrt{\frac{T_1}{T_1}} \cdot \frac{m_1}{m_1} \quad (24)$$

Equation 24 is of now use in this form and can be expressed as follows:

$$\frac{m_3 \sqrt{T_3}}{p_3} = \frac{m_1 \sqrt{T_1}}{p_1} \cdot \frac{p_1}{p_2} \cdot \frac{p_2}{p_3} \cdot \sqrt{\frac{T_3}{T_1}} \cdot \frac{m_3}{m_1} \quad (25)$$

Assuming the bleed mass flow from the compressor to be equal to the fuel flow allows for  $m_1$ ,  $m_2$  and  $m_3$  to be equal [3]. Equation 25 can then be written as:

$$\frac{m \sqrt{T_3}}{p_3} = \frac{m \sqrt{T_1}}{p_1} \cdot \frac{p_1}{p_2} \cdot \frac{p_2}{p_3} \cdot \sqrt{\frac{T_3}{T_1}} \quad (26)$$

### 2.8.2 Impact of ambient conditions on GT performance

A common application of single-shaft GT:s is power generation. The GT is connected to the generator either directly or via a gearbox to match the GT rotational speed to the generator. For a single-shaft machine the rotational speed is constant during all levels of load except of course during start up and



shut down. In figure 8 the compressor no load running line is illustrated. Before loading a single shaft GT the engine accelerates to the designed rotational speed [8].

From eq 26 an increase of  $T_1$  would result in a decrease of the non-dimensional speed. Moving the running line to the left along the x-axis and slightly down along the y-axis in figure 8.

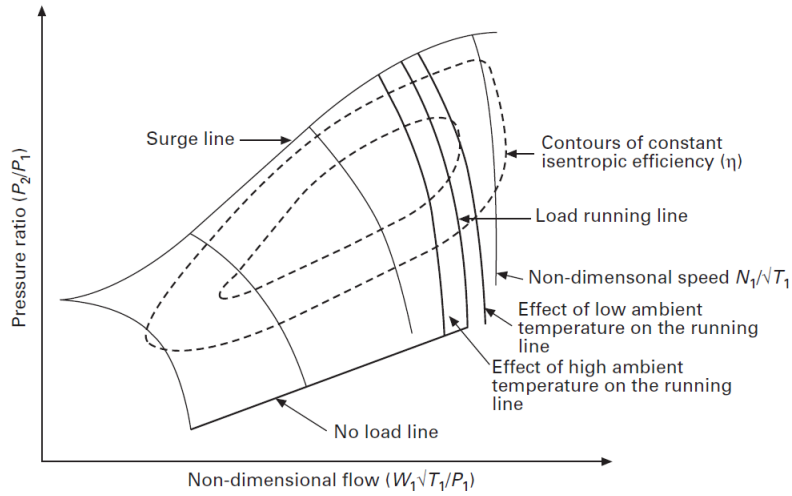


Figure 8: Variations of the Steady state running line of a single-shaft GT due to changes in ambient temperature [8]

## 2.9 Transient operation

Transient operation of a gas turbine can be defined as all operation where engine parameters such as rotor speed, firing temperature or load vary with time. Imagine a GT operating at a steady state, a change in fuel flow would then result in a transient response before stabilizing to another steady state. During this transient response the operating point for the GT leaves the current steady state condition until it has reached the new steady state. Because of this the transient response is characterized with a higher risk of surge [8].

Unlike off design operation a transient response is dependent on how the GT is operated and not the surrounding ambient conditions or faulty components.

Regarding faulty components the transient response offers an opportunity to detect faults at an early stage compared to fault detection during steady state operation. This is due to the performance deviation, caused by the fault, is more likely to be magnified during a start up when compared to the same deviations during steady state. This can be attributed to the increased strain which the components are subjected to during the start. However, faults or deterioration in some components might not affect the steady state performance but instead

lead to a reduced surge margin in the compressor.[9]

### **2.9.1 Startup procedure**

The starting procedure, illustrated in figure 9, is one of the most challenging operation a GT has to perform. The whole engine is initially cranked using a starter motor, usually an electric or hydraulic motor which is in operation until self sustaining speed has been reached. Following section describes how Siemens in Finspong start up their engines.

In order to control the acceleration of the rotor and avoid stall the initial phase of the start is controlled by the STC-signal (Start Controller) from the engine control system. The purpose is to obtain a good starting reliability and make sure the correct fuel flow is achieved before ignition. This is done by limiting the fuel flow according to pre-determined amounts depending on how far the start up procedure has advanced [5].

Purging of the machine takes place soon after the STC is active. This is a procedure where the engine rotates without combustion, the reason for this is to clear the combustion system from remaining air/fuel mixtures which might cause unwanted combustion/explosions. For gaseous fuel powered GT:s this is especially important since gas can more easily leak into the machine when not in operation. The purge procedure is conducted at the same rotational speed as ignition.

Before ignition can occur the starter motor must build up enough mass flow and pressure in the combustion chamber. When this is achieved fuel is injected and ignition occurs. Without the assistance of the starter engine after ignition the gas turbine would coast down resulting in a slow acceleration or even no acceleration. This is due to the low rotational speed which in turn has a negative effect on the compressor efficiency [8].

The STC is in operation until a pre-defined speed when the RUC (Run Up Control) takes over. The RUC-signal limits the acceleration and thermal stresses of the rotor by controlling the acceleration rate of the rotor. Different from the STC the RUC is a closed loop with the rotor speed as a feedback signal which is necessary to maintain control during the acceleration of the rotor. The RUC is active until the rotor speed has reached 6500 rpm where the FLC (frequency load control) takes over [5].

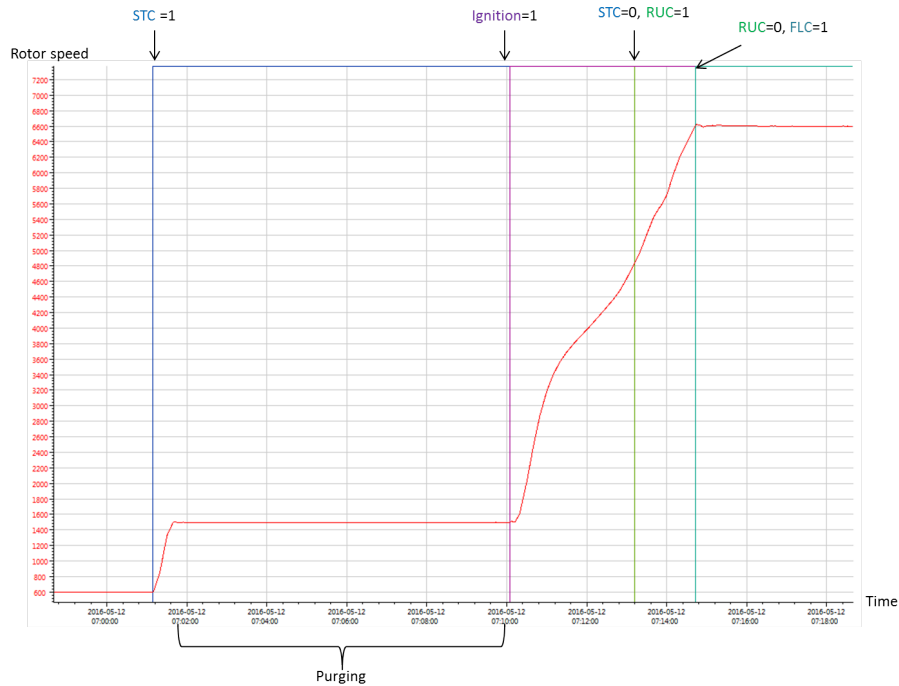


Figure 9: The gas turbine rotational speed (red) is plotted over time along with engine control signals (STC, RUC, FLC) [8]

### 2.9.2 Bleed valve control

The function of bleed valves, is to reduce the flow to the back stages of the compressor, reducing the flow velocity consequently preventing these stages from choking. Avoiding choked flow of the back stages prevents the front stages from stalling. Successful control over the bleed valves can prevent compressor surge during start up or low power operation. The placement of these type of valves are normally along some intermediate stage [8].

The bleed valves are always open during start to reduce the mass flow to the compressor to avoid surge. As the machine ramps up in speed the bleed valves close. During the shut down procedure of the GT the bleed valves needs to open within a second to avoid compressor surge during the roll out [5].

### 2.9.3 VGV control

The use of variable geometry in compressors, such as VGV (variable guide vanes) or VIGV (variable inlet guide vanes), is necessary to control the mass flow through the compressor. The temperature of the flow entering the turbine and the exhaust can then be maintained at some predetermined value with this method. When operating at part load the consequences of controlling the

exhaust temperature this way leads to a reduced flow through the compressor. Thereby the compressor power input is also decreased which is desirable. Being able to maintain the exhaust temperature during low power output at its design value is beneficial for the thermal efficiency, especially if the GT is used in a combined cycle or a heat exchanger is connected to the exhaust [8].

## **2.10 Diagnostics, prognostics and engine monitoring**

Renewable energy constitutes an increasing part of the energy mix and due to its intermittent nature the need for a gas turbine to operate more efficiently and in partnership with renewable energy sources has been amplified. An increased number of starts or increased operating time during part load are factors that can reduce the lifespan of the machine. For the manufacturer to leave guarantees to the operator, regarding performance etc., the development and implementation of a robust and efficient maintenance strategy is vital. A sophisticated maintenance strategy reduces the number of breakdowns, operating costs and downtime [11]. The use of technologies such as the internet of things and the development of sophisticated software have given the GT industry the opportunity to converge their data into a platform, enabling the optimization of fleet monitoring and management. Banks of data containing operational history of the machine can then be accessed and used for diagnostics and prognostics constituting the basis for maintenance decisions.

In light of these technical developments regarding GT monitoring the maintenance strategy have shifted from a "fail and fix" to a "predict and prevent" method. This new method is called condition-based maintenance (CBM) [11].

### **2.10.1 Gas turbine condition monitoring**

It is not uncommon for the GT operator to demand from the manufacturers a guaranteed degradation rate and life cycle costs depending on the use of the equipment. Requirements set by the operator should be met by the manufacturer in long term, global service contracts. To achieve the objectives set by the CBM strategy various monitoring methods can be utilized, presented in figure 10, each with its own advantage [11].

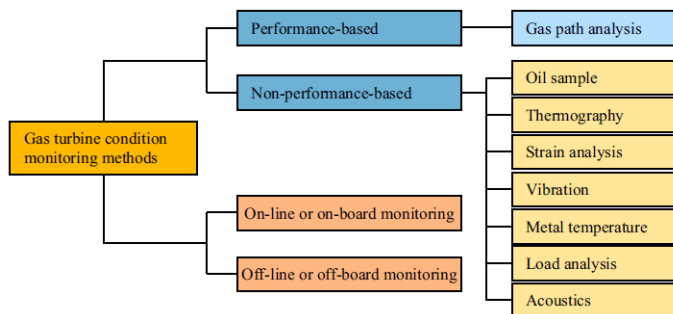


Figure 10: Gas turbine condition monitoring methods

In general gas turbine deterioration can be classified by two categories. Mechanical caused by misalignment, unbalance, loose components, bearing defects and lack of lubrication. The second is aerodynamic performance related problems often caused by compressor fouling, debris deposits, erosion, corrosion. For the latter case the use of performance based monitoring, also called gas path analysis (GPA), provides a cost effective and precise way of predicting impending failures. Explained in depth by Meher [7] the type of problems that manifests themselves as mechanical but in fact have an underlying aerodynamic- or performance based cause. When these are related the problem is categorized as aeromechanical.

Gas turbine monitoring can be performed in two ways, on-line or off-line. On-line monitoring has the advantage of continuously monitor the performance of a GT, the information are used for diagnostic and prognostic purposes in real time. This is a technique that has been adopted in aero engines to track the engine health using satellite feeds. However useful the application of on-line monitoring the technique suffers from high costs and inaccuracy due to measurement data characterized by noise. This noise is the consequence of transmitting the data in real time using wireless technology [11].

Off-line monitoring employs an embedded device that collects data which is then transmitted to an analysis server, the size of the data files are usually large and its therefore common to transmit the data during nighttime. An apparent risk of using off-line monitoring is the possibility that some problem or imminent failure is not detected during the time between data acquisitions. However the advantage of off-line monitoring is lowered costs and accurate collection of data since the data transmission is done without using wireless technologies [11].

## 2.11 Gas turbine performance-based monitoring

When assessing the performance of a GT the concept of gas path analysis (GPA) is often used. Health parameters, such as component flow capacity and efficiency, are used as measuring sticks to appreciate the engine performance. However, these health parameters cannot be measured but when an alteration occurs the measurable variables, such as temperature and pressure, indicates

change. This works due to the thermodynamic correlation between the health parameters and the measured variables and consequently gas-path faults have an observable effect on the performance. To identify the faults a model function and essential data is required [11].

## 2.12 Tools used

### 1. Dymola

Often used during this project is the software Dymola (Dynamic Modeling Laboratory). Dymola is a modeling and simulation tool that is based on the Modelica language.

The Modelica language was developed in 1978 by Hilding Elmqvist for his PhD thesis [2] and is a object-oriented, declarative multi-domain modeling language. The objective was to create a language that could facilitate the exchange of models and model libraries. Modelica uses equations to describe physical systems instead of algorithms for the sake of user friendliness. When the equations for a systems is stated Dymola translates them into code. This can be done in two different ways, either by writing the code yourself in the text mode or by drag and drop of components onto the worksheet in the graphical editor. The graphical editor allows the user to connect several components from a library to create models which is appropriate for users with little experience. A new model can be created from scratch using components from a standard library or an existing model can be remodeled or updated by using new components or writing new code. In addition to the two modeling modes a simulation mode exist where the user can test the model created and plot potential output data.

### 2. STA-RMS and RMSview

STA-RMS (Siemens Turbomachinery Applications - Remote Monitoring System) is a database consisting of measured data from all the Siemens gas turbines in operation. It's an off line system where data is uploaded daily. RMSview is the software used to view and extract data from STA-RMS.

### 3. DMA

DMA (Daily Monitoring Automation) is a software developed by Siemens which enables the user to program agents for managing large amounts of data extracted from STA-RMS. The interface is graphical where the programming of the agents is done by connecting one or several function boxes. The data handling process, by DMA, can be considered more of a filtering of the data than an extraction of data since the programming structure is built around a constant stream of information.

### 4. Excel

Is a spreadsheet software which features calculation, graphing tools, pivot tables, and a macro programming language called Visual Basic for Applications (VBA).

## 5. **Matlab**

Matlab is a programming language developed by MathWorks. Matlab is primarily intended for numerical computation but allows for matrix manipulation, plotting of functions and data and implementation of algorithms. [12]

## 3 Methodology

This chapter describes the work process, what steps have been taken and the reasoning behind the decision making during the work process. It includes information about the modeling of the fuel- and bleed valves, how they were implemented in the complete model of the SGT-800. The process of collecting data will be explained along with a description of what data is of interest.

### 3.1 Literature study

A literature study has been conducted with the purpose of examine if any similar work has been done previously. The literature study have been ongoing during the first half of this project, providing information about transient operation and diagnostics. The papers have been organized and rated depending on relevance to make it easier to go back and find further information. Most papers were found externally.

### 3.2 The SGT-800 transient model

Figure 11 shows the graphical layout of the SGT-800B1 transient model developed by Siemens. The two parts of interest for this project are the fuel system, marked in red, and the core engine, marked with green. Input data such as fuel pressure, ambient temperature and pressure for the model can be entered in the yellow box in the top left corner.

The governing equations of the fuel- and compressor bleed valves have been updated in order to reflect the valve characteristic of the valves being used in the SGT-800. If this solution is not satisfactory with respect to the model performance, such as simulation time, accuracy etc, the fuel- and bleed valves implemented in the transient model will be replaced with a standard model compressible valve. The reason for using a standard library valve is the possible reduction in simulation time and the freedom of input parameters.



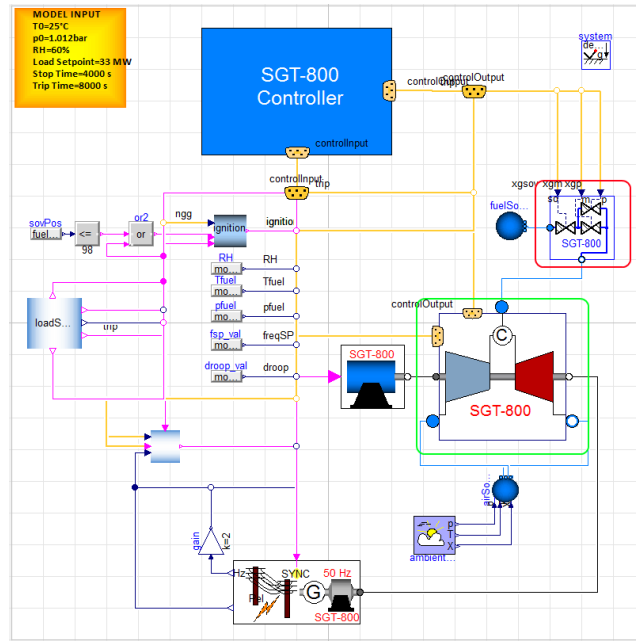


Figure 11: The Dymola model of the SGT-800B1, the red box indicates the fuel system and the green box indicates the engine containing the bleed valves

### 3.2.1 Fuel valve model

The original fuel system is illustrated figure 12. This model employs a valve that calculates the effective area, in the flow direction, with equations based on the manufacturers valve characteristics. The new valve, illustrated to the right in figure 13, has an advantage compared to the old valve. More functions is packed in the new model valve and the flow characteristics of the valve are not determined by equations and can be changed more easily depending on the application.

### 3.2.2 Old valves

The original valves, circled in red, receives an input signal in the form of what percentage the valve should open (open fraction). From this information the equations visible in the text mode of the valve will then calculate the effective area and consequently the mass flow. This valve model utilizes a library constructed by Siemens where the only difference between the main and pilot valve is the valve characteristic equations, however the adjustment possibilities of this type of valve model is limited.

To provide a reference point for the new Modelica valves the original valves were updated in regard to their valve characteristics from data provided by the manufacturer.

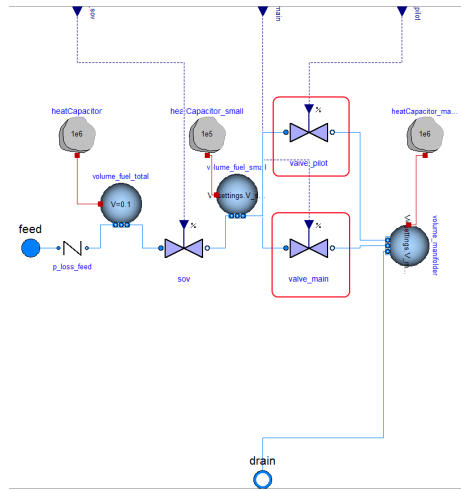


Figure 12: The original model of the fuel system

### 3.2.3 New valves

The valve model, in figure 13 circled in blue, are the new valves which is part of the Modelica standard library. The use of the new valves introduce the possibility to make several adjustments to the valves such as adding a signal filter or change the valve characteristic etc. This is provides an advantage when modeling because the same valve can the be used for several applications in the model.

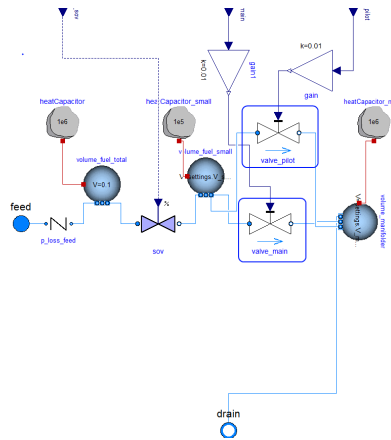


Figure 13: The fuel system, equipped with the new valves

### 3.2.4 Bleed valve modification

The original bleed valve used in the model can be considered as a piece of tubing having the ability to control the mass flow, operating without pressure loss. This of course is an estimation that has worked fine but for increased accuracy further development and real valve adaptation is necessary. The updated version of the valve model, seen in 14, include the same type of valves used in the fuel system, these are marked in green. Two SGT-800B1 has two bleed valves.

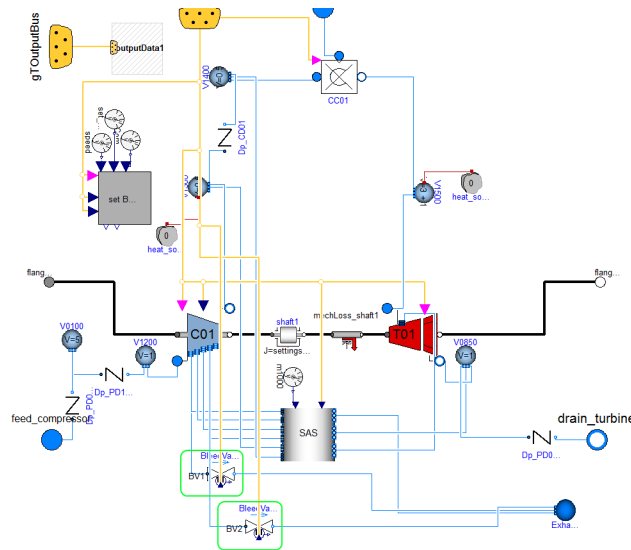


Figure 14: The Dymola model of the compressor and turbine components, the bleed valves are circled in green

## 3.3 Data collection

Since the purpose is to develop a method of assessing the GT health during transient operation, the data points chosen for comparison is only relevant during start and stop of the GT. This section explain what data have been collected, why these data point are of interest during the start and how the data have been collected. All data points are in this case temporal intervals between the start of an event until the end, except data point seven which is the accumulated deviation of the bleed valves from their set point.

### 3.3.1 Data points

The numerated sections below describes the data points collected from STARMS. Some of the temporal intervals have been highlighted in figure 15, where a successful start up process is plotted from actual data along with the relevant engine control signals.

1. *Duration from main flame signal until RUC in operation signal is activated, figure 15.*

This interval is indicative of how the machine is operated during start and provides information of how fast the machine is accelerated after ignition. The consequence of an engine accelerating too fast during start is a reduced surge margin and subsequently surge.

2. *Duration from RUC in operation until the release of the starter motor, figure 15.*

This data point supervise the transition between the STC and RUC-signals. An incorrect fuel flow of the STC would result in the an incorrect fuel flow at the release of the starter motor. This in turn would result in an increased duration between the RUC-signal and starter motor release.

3. *Duration needed for the bleed valves to close during start.*

The SGT-800 has two bleed valves, data will be collected for both valves. In order to detect if the valve is stuck the closing time is supervised. A bleed valve that is stuck or resist during closure may cause harm during roll out of the engine.

4. *Duration needed for the bleed valves to quick open during stop.*

If a GT is part of the base load production it is common that the operating periods between starts can be long. When stopping a GT after a long period of operating time the valves might exhibit difficulty opening. This is due to the high operating temperatures and pressures the valves have been subjected to for this period. An increase in the bleed valves opening duration would indicate a worn or stuck valve and is therefore supervised.

5. *Duration of the rotor speed to reach purge speed from the Purge signal is activated, figure 15.*

Resistance during the start can indicate a bent rotor. It is advantageous to detect this as soon a start is initiated since the consequences of a bent rotor are more severe the higher the rotational speed.

6. *Roll out duration of the GT after a stop or trip.*

The inertia of the rotor in a SGT-800B1 is constant. The time to roll out the rotor to barring speed should therefore also be constant. A decreased roll out duration would indicate resistance to the rotor, possibly the rotor touching the casing or a worn bearing.

7. *The accumulated deviation of the bleed valves from their control set point.*

This data point measures the deviation between the set point and the actual open fraction. The deviation is then accumulated for every measurement acquired from the data. If the bleed valve has problem following the set point signal (from the engine control system) it indicates that it

may experience resistance during operation. The resistance may increase with time and cause more acute problems at the next start or stop.

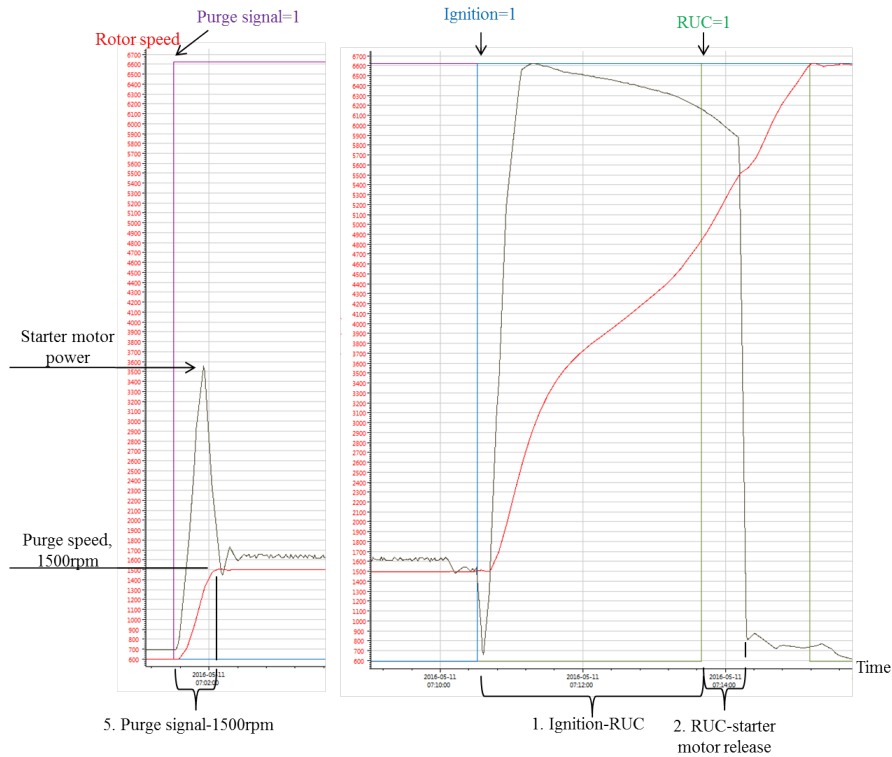


Figure 15: The start up process for Denizli 1. Rotor speed is plotted against time, binary signals from the control unit is plotted at different stages during the start.

### 3.4 Chosen sites and data collection interval

The reasoning behind what sites should be studied during this project were dominated by the desire to collect data from sites that differ in ambient conditions, number of operating hours and variations in start/stop frequency. The reason for studying more than one GT at some locations is to evaluate any differences between the GT start up procedure regardless of ambient conditions. The time period during which the data have been collected differs slightly between sites since some sites have not been in operation for more than a few years. The time period initially chosen for the data collection are the total operating time of different sites. The power production of some sites varies a lot, consequently the amount of starts and stops are more frequent, resulting in an

increased amount of data points for some sites. Following sites were chosen for the data collection:

- Amata Rayong 1, Thailand. High ambient temperatures along with high relative humidity.
- Denizli, Turkey. A site characterized by very high start/stop frequency.
- Frankfurt X2, Germany. ISO site with high number of operating hours.
- Frankfurt X3, Germany
- Termoelectrica del Sur 1 (Tds1), Bolivia. Located at a high altitude with high start/stop frequency
- Termoelectrica del Sur 2 (Tds2), Bolivia
- Namyangju, South Korea. Average site which is subjected to all seasons
- JSC Yamal 1,2,3,4, Siberia. An extremely cold site

### **3.5 Manual data collection**

The objective of this process were to compile collected data together with the simulated data in order to analyze the difference. Additional use of this manual data collection was to act as a reference dataset when designing the automated data collection agents in the next step. This was done in order to assert the agent validity when collecting correct data. The ambient conditions of every data point were collected and used to run the transient model to produce the simulated data.

### **3.6 Automated data collection and screening**

To provide a considerable basis for evaluation regarding the start up procedure for the chosen sites the data collection has to be extensive in order to demonstrate deviant data points. Following section will present the work conducted previous to the automated data collection. The software DMA (Daily Monitoring Automation), developed by Siemens, were used during the extraction of data. For this project the software were used to program macros to extract the desired data over the specified period of time. The data were then presented in a spreadsheet fashion. Further analysis of the extracted data included the development of a MATLAB script in order to present the data in a scatter diagrams and calculate the average values and standard deviations.

#### **3.6.1 Macro working principle**

Following section explains the general function of a macro, illustrated in figure 16, implemented in the software DMA (Daily Monitoring Automation). Some macros are different in their construction since additional signals is necessary to identify the temporal intervals of interest but the principle remains the same.

- *1. Data input*  
The "Tag readers" imports data for the specified tag from the STA-RMS data base. In this case the GT rotor speed, STC signal and main flame signal is imported.
- *2. Data collection conditions*  
When collecting data the desire is to only collect data during time periods of interest, eg. during starts or stops. However, when running a macro through several years of data it is necessary to incorporate conditions that specifies when the agent should be active. This macro is only active when rotor speed is less than 6000 rpm, the STC is in operation and main flame is activated.
- *3. Logical AND operator*  
When all the inputs are activated simultaneously the AND operator will deliver a boolean to signal that all the conditions are fulfilled. This in turn signals the temporal counter in step 4 to activate.
- *4. Temporal counter*  
Since the interest of this project is to examine different time intervals during a GT start a temporal counter has been implemented in this macro. This counter starts counting when the output signal from the AND operator is binary. This is also the output of the macro.

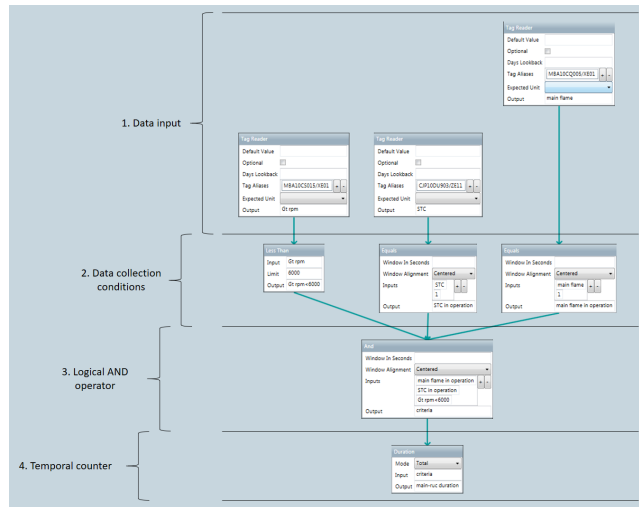


Figure 16: Layout of data point 1

### 3.6.2 Agent development

For every data point described in section 3.3.1 a macro has been developed. Additional macros that were necessary for the data collection were developed.

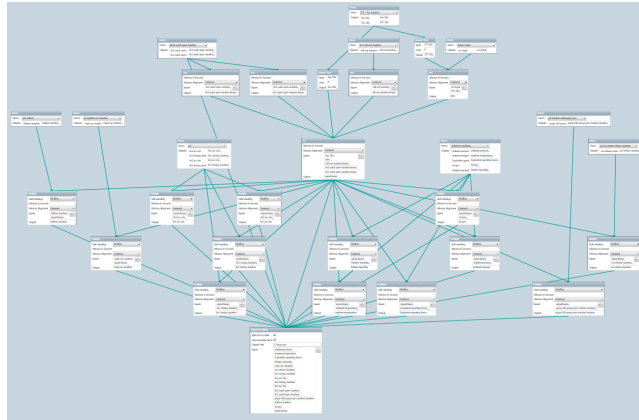


Figure 17: The finished agent used during the automated data collection

These include functions which dictate when the macros developed for the data points should activate. E.g. when the tag reader reads the data for a specific data point, if not processed properly, the output data will also include all the instances where the duration is zero. The reason for limiting the activation of the macros is because the actual time needed for data collection will increase significantly if the macros are able to continuously collect irrelevant data.

One agent was developed in order to implement all of the macros together. The reason for this was to facilitate the data collection and provide a single output file. The working principle of the agent is similar to the macros but provides a single output file containing the data from all of the data points. The finished agent can be seen in figure 17.



## 4 Result

In this section the results produced during this thesis will be presented in chronological order.

### 4.1 Transient model valve update

This section presents the results from the model modifications made to the transient model in Dymola. Schematic images of the model will be omitted since they have already been presented in the method section.

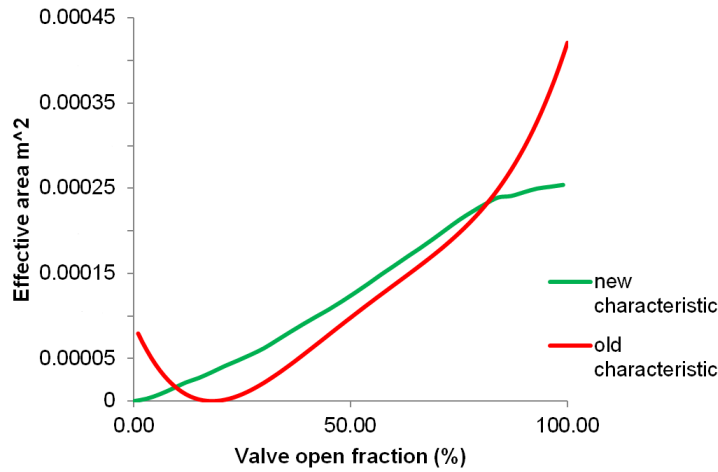


Figure 18: Difference between the old and updated bleed valves

Figure 18 shows the difference in the flow characteristic for the old- and updated bleed valves. As mentioned in section 3.2 the new characteristic have been collected from the valve manufacturer specifications and can be considered correct compared to the old valve characteristic. Line estimate has been used in order to produce the equations. The fuel valves updated characteristic have been omitted since the graphs in figure 18 can be considered explanatory for both type of valves.

Following equations were used for the updated valve characteristic, provided in table 4.1 are the coefficients used in equation 27, 28, 29,  $x$  is the open fraction.

$$BV = a + b * x + c * x^2 - d * x^3 + e * x^4 - g * x^5 \quad (27)$$

$$Main = -a + b * x - c * x^2 + d * x^3 - e * x^4 + f * x^5 \quad (28)$$

$$Pilot = -a + b * x + c * x^2 - d * x^3 + e * x^4 - f * x^5 + g * x^6 \quad (29)$$

coeff.	BV	Main	Pilot
a	$2.00114265463958E^{-7}$	$4.51058385607492E^{-6}$	$2.07311496301795E^{-7}$
b	$4.03674298625647E^{-4}$	$1.88943086798411E^{-6}$	$1.05895289356151E^{-7}$
c	$3.86861398434639E^{-5}$	$7.08616044211224E^{-9}$	$8.28132774620058E^{-8}$
d	$1.93055484969422E^{-6}$	$5.56580057492260E^{-9}$	$2.86923325358669E^{-9}$
e	$4.05276413435617E^{-8}$	$8.16954640035557E^{-11}$	$5.75242140137369E^{-11}$
f	$2.55400834256707E^{-10}$	$4.20524451587751E^{-12}$	$5.19739547490065E^{-13}$
g			$1.63296370245219E^{-15}$

Table 1: Coefficients used in equation 27, 28, 29

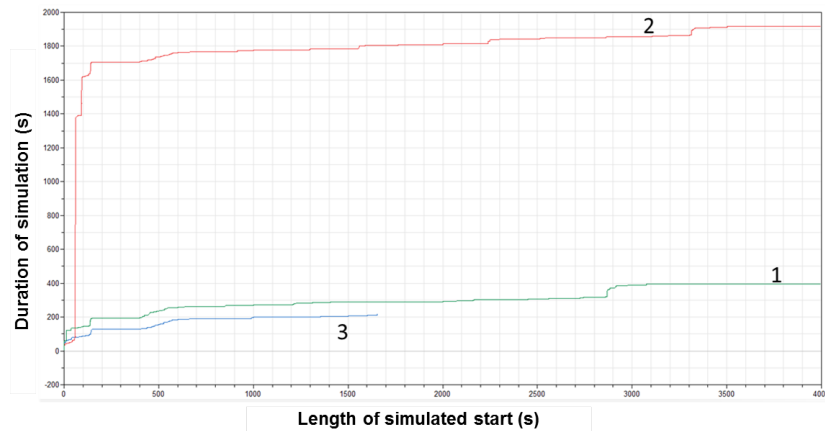


Figure 19: Simulation time for the transient model with three different valve setups.

In figure 19 three graphs are visible showing the simulation time for the following scenarios:

1. Old valves with updated equations.
2. Bleed valves and fuel valves have been replaced with the Modelica standard valve.
3. The bleed valves have been replaced with a Modelica standard valve. The fuel valves have updated equations.

From figure 19 it can be seen that the simulation time is significantly higher for scenario two than the other scenarios. Scenario three displays the lowest simulation time until the simulation were interrupted. What is not visible by the graphs is the flexibility of the model during the different valve setups. The model were significantly more flexible and able to continue calculation regardless of input data for scenario one.

## 4.2 Manually collected data points

Following scatter plots have been produced with Excel in order to assess the difference in behavior between the model and collected data. Roughly 500 measuring points have been collected and simulated. Some of the plots might appear to have missing data where gaps are visible between measurements. This is due to unsuccessful starts or stops where the collected data have been removed because of incomplete data. The x-axis is of little importance since it displays only the date when the data was collected. Data point seven has not been collected or simulated during this process. The reason for this is because data point seven were not initially a data point of interest and has therefore only been examined during the automated data collection.

The data points presented in this section has been collected from the following sites:

- Amata-Rayong, Thailand
- Namyangju, South Korea
- Denizli, Turkey
- Frankfurt X2, Germany
- Termoelectrica del Sur 1, Bolivia
- JSC Yamal, Russia

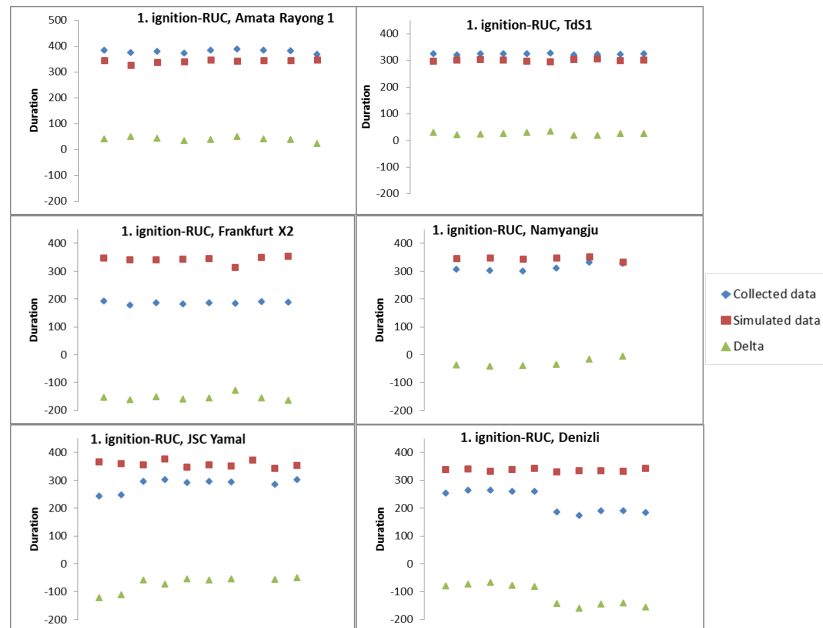


Figure 20: Data point 1. Duration from ignition (main flame) until (RUC)

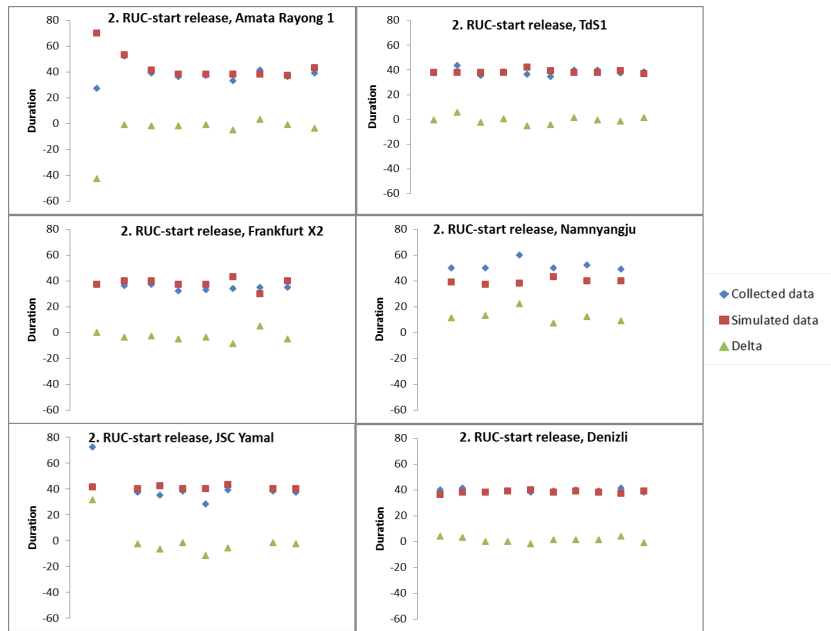


Figure 21: Data point 2. Duration from RUC until release of starter motor.

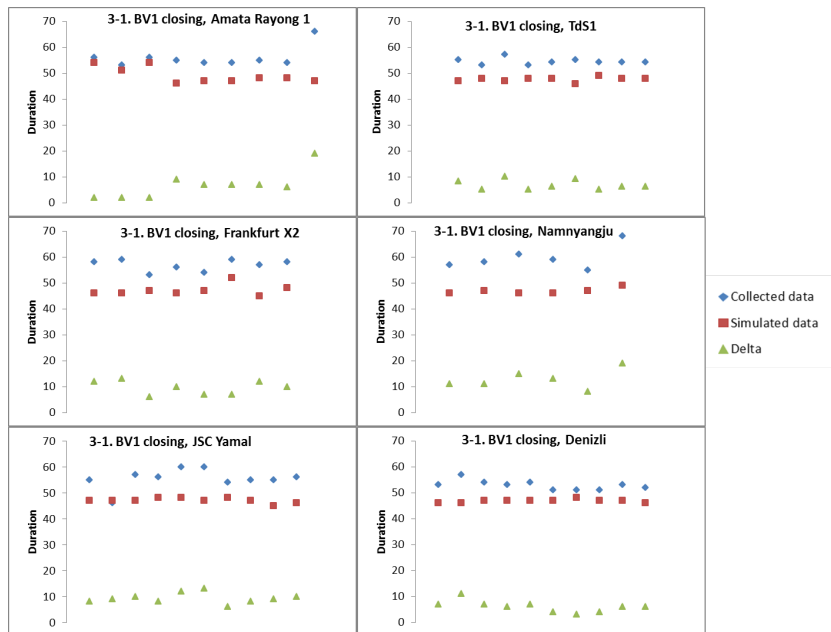


Figure 22: Data point 3. Duration for Bleed valve 1 (BV1) to close during start.

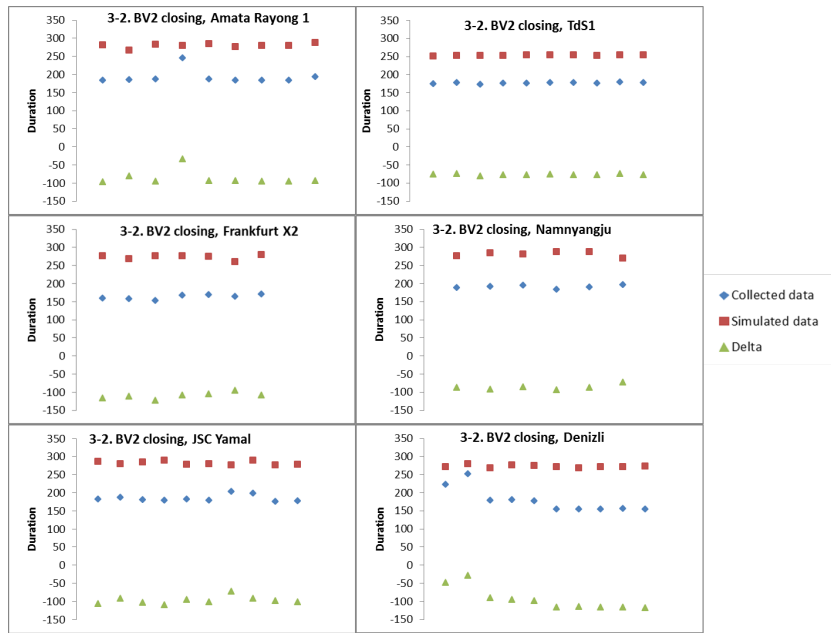


Figure 23: Data point 3. Duration for Bleed valve 2 (BV2) to close during start.

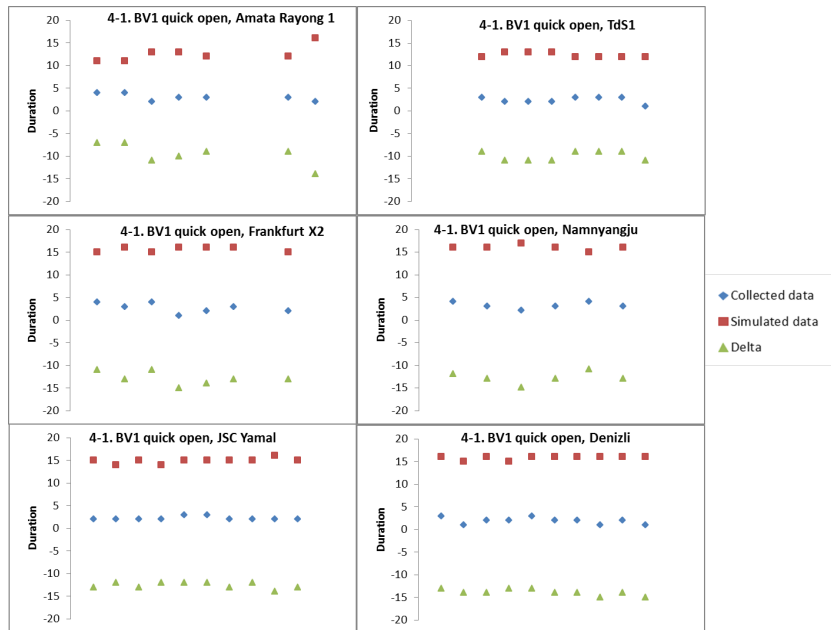


Figure 24: Data point 4. Duration for Bleed valve 1 (BV1) to open during stop.

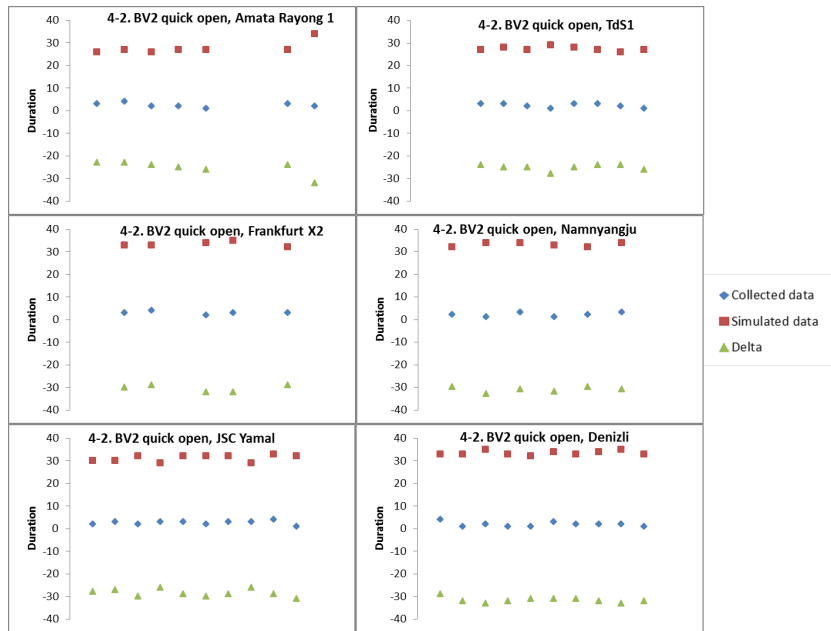


Figure 25: Data point 4. Duration for Bleed valve 2 (BV2) to open during stop.

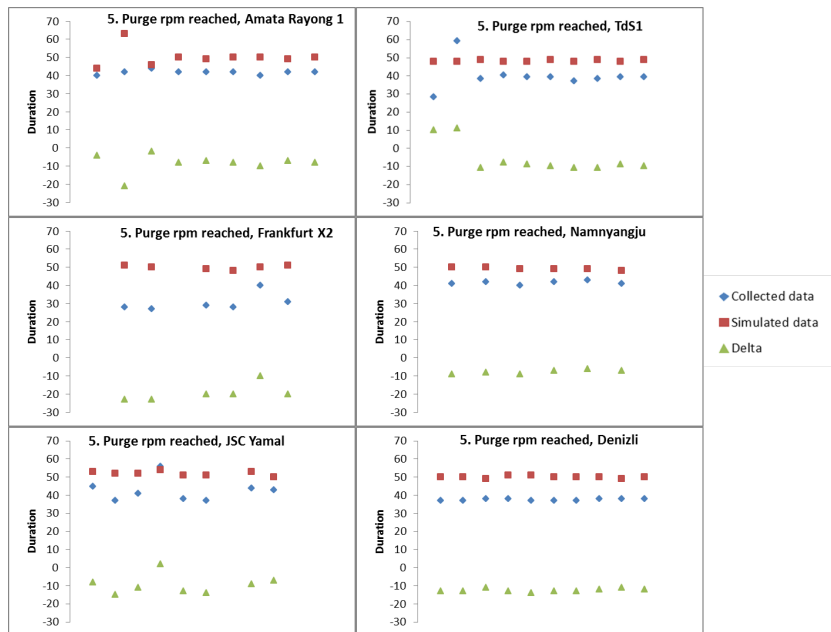


Figure 26: Data point 5. Duration of the rotor speed to reach purge speed.

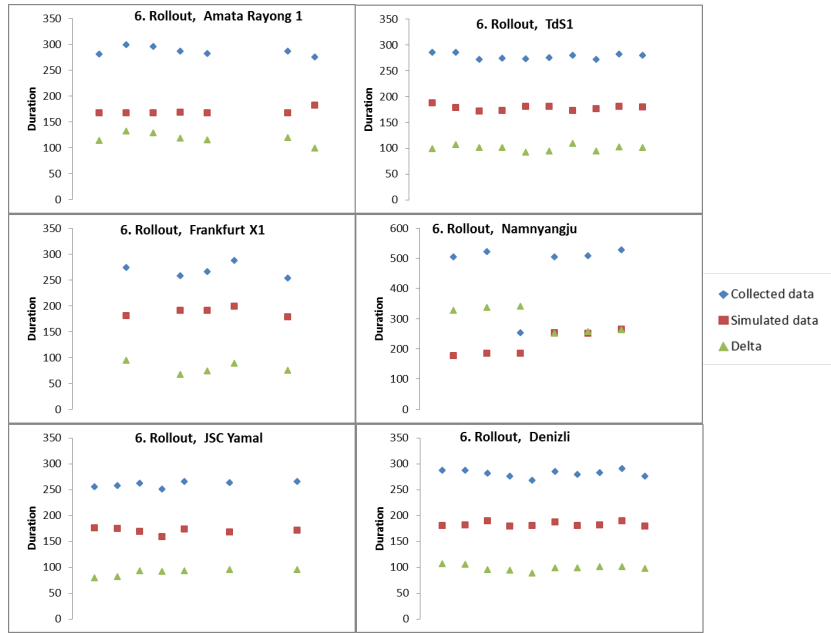


Figure 27: Data point 6. Roll-out duration of the rotor after a stop.

### 4.3 Automated collection of data points

Following scatter plots have been produced with Matlab. The scale of the y-axis have been adjusted to more clearly display the dispersion of the data. Alla data have been plotted against temperature and equivalent operating hours. The option to plot the data against ambient pressure and relative humidity have been investigated. As expected these plots displays an identical dispersion as when plotted against ambient temperature and have therefore been omitted from the result.

## Data point 1

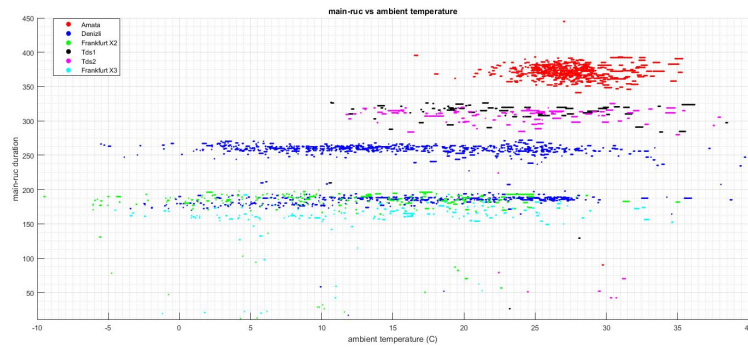


Figure 28: Data point 1, Duration from ignition (main flame) until (RUC) plotted against ambient temperature

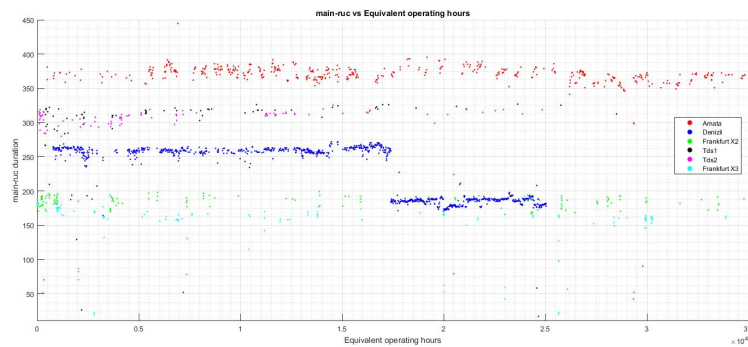


Figure 29: Data point 1, Duration from ignition (main flame) until (RUC) plotted against equivalent operating hours

In figure 28 an apparent element of the data is the double fields illustrated by the Denizli data (blue). The same data set is illustrated in figure 29 where an apparent change in duration happens at 17000 equivalent operating hours (EOH) for the Denizli data.

The main-ruc duration seems to be very site dependent and not sensitive to the ambient temperature. All of the data sets were also plotted against ambient pressure and relative humidity but demonstrated no dependency, similar to figure 28.



## Data point 2

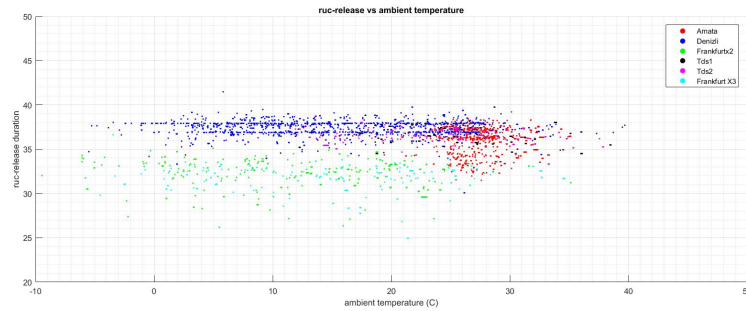


Figure 30: Data point 2, Duration from RUC (main flame) until release of starter motor. Plotted against ambient temperature

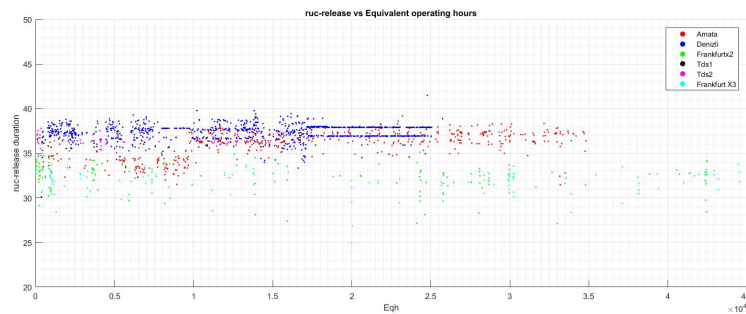


Figure 31: Data point 2, Duration from RUC (main flame) until release of starter motor. Plotted against equivalent operating hours

In figure 30 none of the data sets displays a temperature dependent behavior. The Denizli dataset displays two lines from the data dispersion, visible both in figure 30 and 31. At 10000 EOH in figure 31 the Amata data set (red) has a slight increase in duration.

### Data point 3

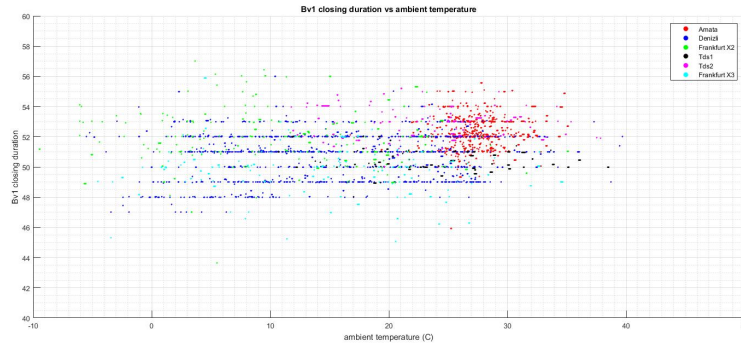


Figure 32: Data point 3, Duration for Bleed valve 1 (BV1) to close during start, plotted against ambient temperature

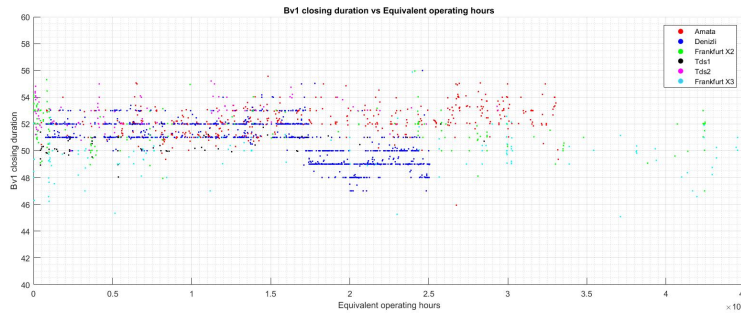


Figure 33: Data point 3, Duration for Bleed valve 1 (BV1) to close during start, plotted equivalent operating hours

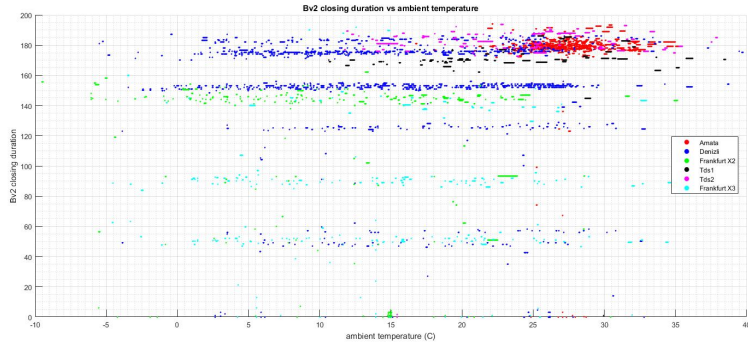


Figure 34: Data point 3, Duration for Bleed valve 2 (BV2) to close during start, plotted against ambient temperature



Figure 35: Data point 3, Duration for Bleed valve 2 (BV2) to close during start, plotted equivalent operating hours

Noticed for data point 1 in figure 29 the Denizli data set displays a clear change at 17000 EOH. This can be observed to happen in figure 35 and 33 also. The data have less variation onwards especially for BV2 displayed in figure 35. The Frankfurt X3 data set displays two lines in figure 35 at 50 and 90 seconds, similar behavior to the Denizli dataset but without any clear change when observed in figure 35 plotted against equivalent operating hours.

## Data point 4

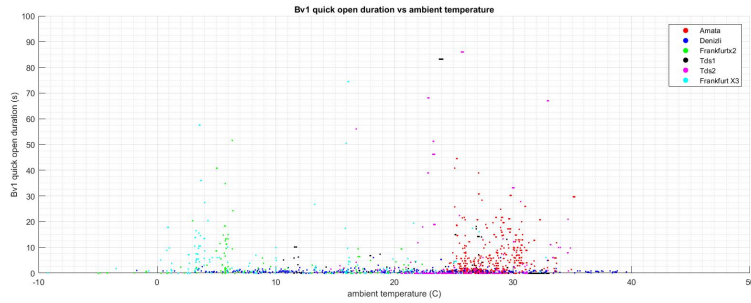


Figure 36: Data point 4, Duration for Bleed valve 1 (BV1) to open during stop, plotted against ambient temperature

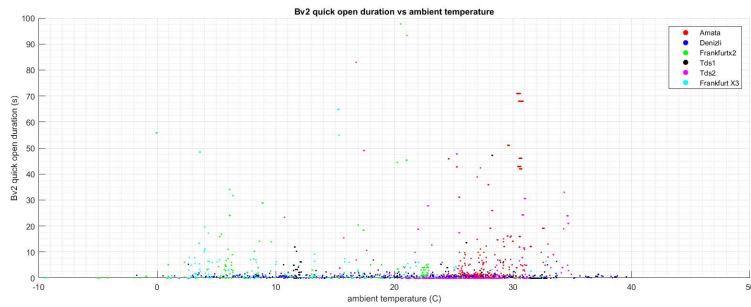


Figure 37: Data point 4, Duration for Bleed valve 2 (BV2) to open during stop, plotted against ambient temperature

Mentioned previously in the theory section the bleed valves needs to fully open within a second after the set point signal is changed. In figure 36 and 37 it is clear that a substantial share of the data points, regardless of site, have a larger duration than one second. This is an unreasonable result and further explanation will be presented in the discussion section. For this reason data point 4 have not been plotted against equivalent operating hours.

## Data point 5

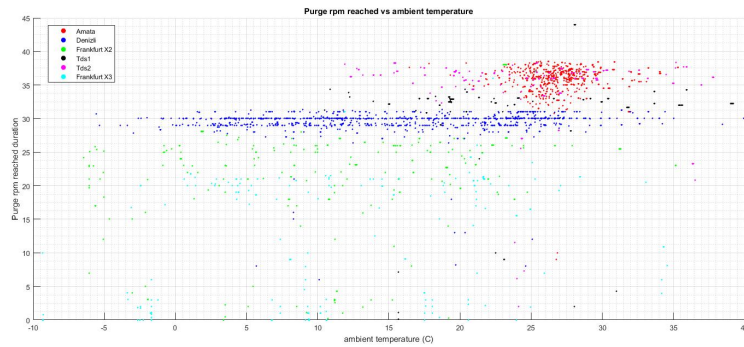


Figure 38: Data point 5, Duration for the rotor speed to reach the purge speed after purge signal activation, plotted against ambient temperature

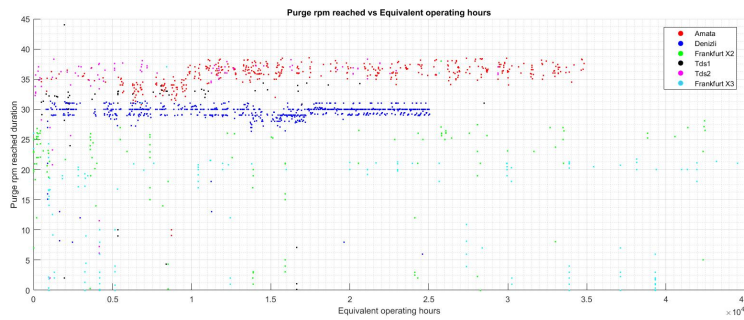


Figure 39: Data point 5, Duration for the rotor speed to reach the purge speed after purge signal activation, plotted against equivalent operating hours

For the Denizli dataset in figure 38 and 39 some lines are present in the graph, this will be discussed in section 5. The duration is higher for the Amata Rayong and TdS1 site. The two datasets for Frankfurt generally exhibit a lower duration and several measurements can be observed to be unreasonably low.

## Data point 6

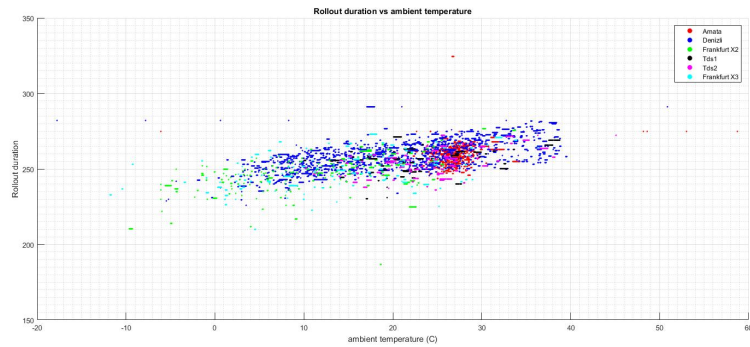


Figure 40: Data point 6, Roll-out duration of the rotor after a stop. Plotted against ambient temperature

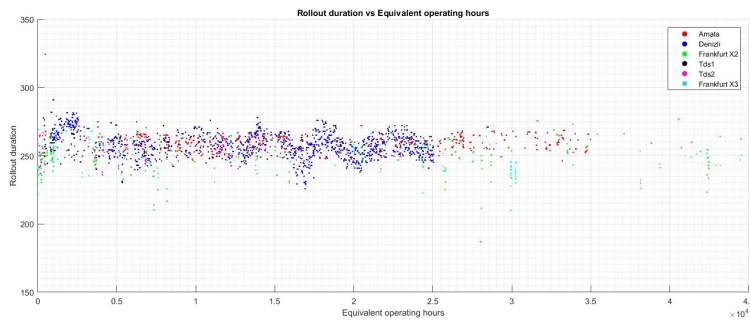


Figure 41: Data point 6, Roll-out of the rotor after a stop or trip. Plotted against equivalent operating hours

In figure 40 and 41 the dispersion of the data is less. A few data points can be identified to be unreasonable and will be explained in the discussion section. An increase of the roll out duration can be identified with increased ambient temperature.

## Data point 7

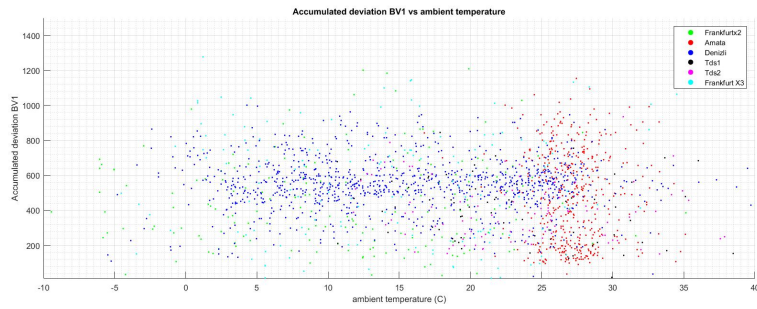


Figure 42: Data point 7, Accumulated deviation of Bv1 from its set point. Plotted against ambient temperature.

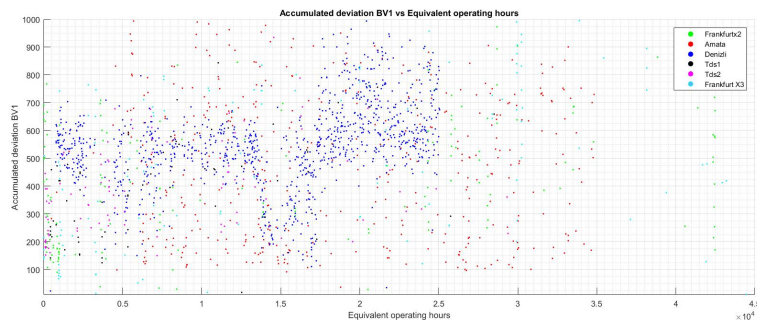


Figure 43: Data point 7, Accumulated deviation of Bv1 from its set point. Plotted against equivalent operating hours

Considering figure 42 the dispersion is constant. In figure 43 the Denizli dataset is the only dataset indicating a noticeable difference at 15000 EOH.

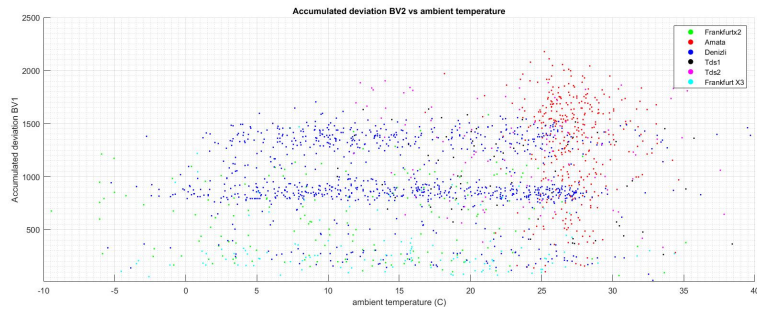


Figure 44: Data point 7, Accumulated deviation of Bv2 from its set point. Plotted against ambient temperature.

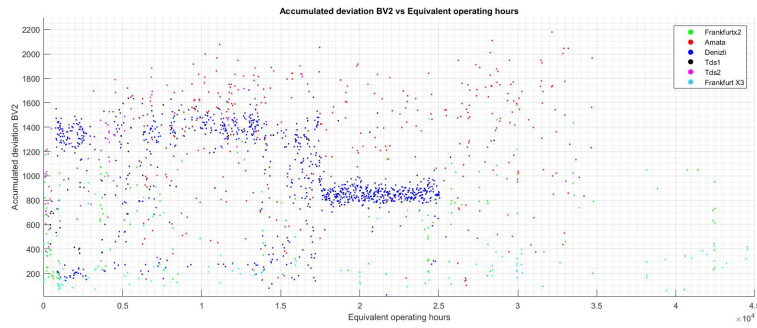


Figure 45: Data point 7, Accumulated deviation of Bv1 from its set point. Plotted against equivalent operating hours

In figure 44 the dispersion of the data for the Denizli dataset is constant but grouped together in two fields. Figure 45 illustrates a change for the same dataset at 17000 EOH where the data is more grouped together.



## 5 Analysis

This project has contained three major parts during the execution, the transient model valve update, the manual collection of data and the automated collection of data. The idea being to first update the model to reflect the actual valves used, this was done so the transient model could produce correct simulations when compared to the collected data. However, the development of the agents proved to consume more time than expected, also the transient model was not implemented into the software DMA at the time of the data acquisition. Consequently the transient model was only used when operated manually leading to no simulated data available to be compared during the automated data collection.

### 5.1 The valve model update

In order to make the transient model more precise in regard to the bleed- and fuel valve flow characteristic these were updated. Initially the intent were to replace the old valves with a Modelica standard valve which theoretically would make the model easier to adjust for different simulation purposes. The result from the modeling clearly shows that the simulation time for the original valves is much less, 1800 seconds for scenario two and 300 seconds for scenario 1, seen in figure 19. This is not an acceptable increase of simulation time since it would make the model impractical, especially since everyday use of the model probably would include multiple simulations daily.

The third scenario displays a shorter simulation time until it is interrupted. This could indicate that the model simulation time might be decreased using the Modelica valve for only the bleed valves. However, several attempts were made to avoid the model from crashing, without success, rendering this setup unusable for model use. The model seemed prone to crash when the characteristics of the Modelica valves were changed, e.g. when changing from a linear to a quadratic characteristic. This is unfortunate since that feature of the valve were one of the main reasons to update the model. However, the effort involved in updating the old valve flow characteristic equations proved to be acceptable and perhaps this may be a reasonable way of updating other valves.

### 5.2 The manual data collection

In this section the scatter plots presented in section 4.2 for the manually collected data will be analyzed. The model was validated using the same ambient conditions for the observed start in RMSview.

#### Data point 1, duration from ignition to RUC

It is evident that the the model never succeed to simulate the exact behavior observed from the collected data. For data point one, in figure 20, the duration is sometimes higher than the simulated data (Amata Rayong, TdS1) and for other sites it is less. The biggest difference can be observed for Frankfurt X2

where the duration for all measurements is around 200 seconds. The acceleration is dictated by the STC-signal which specifies the amount of fuel input during the first phase of the start. These fuel specifications cannot be changed and variations of data point 1 is therefore likely to depend on an incorrect fuel valve characteristic. Another reason for these variations is the type of fuel used. The quality of fuel might vary (different LHV) depending on site and this could then result in a more rapid start when using a more potent fuel (higher LHV). For the Denizli site a decrease in duration can be observed for the collected data. Similar to the Frankfurt site this might also be an effect of variations of the LHV of the fuel.

Generally observed from all the graphs is a dispersion of the average values of the collected data. Ideally should the duration for the collected data exhibit the same constant behavior as the simulated data. Section 2.9.1 mentions that the STC-signal is an open loop, meaning it cannot detect deviations of the fuel valve characteristic. Evident from the result is that data point 1 pick up the variations of the duration from ignition to RUC. Making data point 1 suitable for monitoring discrepancies in the control system settings.

#### **Data point 2, duration from RUC to starter release**

From an initial observation of all the graphs in figure 21, the delta can be confirmed to hover around the zero value in an almost constant manner. This is either an indication that the model is more accurate or that the collected data can be considered to vary less. For future use in a monitoring system this would indicate that a deviant measure could be identified by this data point.

For the Amata Rayong site a deviant simulation measure can be observed. This can be considered as a unreasonable value since the input data for the model does not differ significantly from the rest of the simulated data. This measure could therefore originate in operator blunder or incorrect model settings.

#### **Data point 3-1, BV1 closing duration**

Similar to the previous data point, the collected data in figure 22 varies less and the duration is longer than for the simulated data. For all of the sites the model provides constant data even though it is not sensitive to variations apparent in the collected data. Considering the last collected data measurements for site Amata Rayong and Namnyangju, they are considerably higher than the rest of their respective dataset. As mentioned in section 3 this increased duration might be due to resistance in the valve mechanism. This could possibly provide a relevant data point for future use when assessing a GT start up procedure since differences between collected and simulated data can be observed.

#### **Data point 3-2, BV2 closing duration**

The simulated duration in figure 23 is here constantly higher than the collected data. Similar to previous results the model is not sensitive to the variations

experienced in the collected data. However, since the scales are different for this data point the question can be raised of how a variation for data point 3-2 would correspond to a deviant measure.

#### **Data point 4-1 and 4-2 BV1 and BV2 quick open duration**

The simulated duration visible in figure 24-25 is longer than for the collected measurements. This is likely due to the model not being capable of simulating such a quick response or that perhaps the model was not correctly adjusted during the simulation. For the Amata Rayong site the last simulated measurements are longer for both BV1 and BV2. The collected duration is around 5 seconds or less, for both valves, which can be considered a normal duration for a fully working bleed valve.

#### **Data point 5, Purge speed reached duration**

Some difference between the sites can be noticed in figure 26. The Denizli and Namyangju dataset have less variations compared to the data presented in the other plots. Similar to some previous results are that the simulated duration is longer than the duration from the collected data.

#### **Data point 6, Roll out duration**

Not surprisingly is all of the collected data for this data point within reason except the duration for the site Namyangju. Illustrated in figure 27, the average duration of this site is about 500 seconds compared to 300 seconds for the other sites. This is due to a decreased barring speed of 200 rpm. All of the other sites have a barring speed of 600 rpm. Otherwise does the model provide constant output data, of around 175 seconds, regardless of site tested. As mentioned for data point 4 this might be due to incorrect settings of the model during simulation.

### **5.3 The automated data collection**

The validity of the agents used during the automated data acquisition will be discussed along with the agent development and implementation. As mentioned in section 3 the transient model were at the time of data acquisition not available in the DMA software, the comparison between the collected data and model data has therefore not occurred. The result from the automated data collection is then discussed from the potential it may bring when applied in conjunction with the transient model. This section analyze the results presented under section 4.3.

#### **5.3.1 Agent/macro development and implementation**

This project of developing macros to collect data from STA-RMS were of major extent during this process. The development took place as an initial step where

one agent were developed to collect all the data of interest. Since the software DMA uses nested macros, a macro had to be developed for every data point of interest. Additional macros had to be developed in order to program the agent to collect only the data of interest and discard irrelevant data. This was necessary in order to limit the data size and provide files ready for processing. The macro development proved a time consuming task since every macro had to be tested over a time period and then approved for further data collection. Since the time intervals that were examined for the different sites were between four to nine years the data acquisition itself proved time consuming. The data acquisition could take up to five days for all the data points.

Due to some parameters of the macros not being correctly adjusted several irrelevant data points were collected. The reason for not detecting this is probably because the data acquisition were substantially higher, and more starts were examined, than during the testing of the macros.

The irrelevant data is visible in the majority of the scatter plots produced during the automated data collection process. E.g. for data point 1 (ignition-RUC duration), in figure 28, a clear diversity of the duration is visible depending on site. Several durations from the collected data have an unreasonable value of around 100 seconds or less. To achieve this, the acceleration of the GT would have to be unreasonably fast. Similar deviant data can be seen for all data points except data point 6, in figure 40, and is most likely to be related to improper adjustments of the macros implemented in the agent. For data point 6 the dispersion is much less and the deviant measurements are present to a lower degree. For this data point it is the roll out duration that is measured and what is of interest is the ability to detect durations below a reasonable value since this would be indicative of rotor resistance. The macro used for the data collection for data point 6 seems to provide reasonable output data. However some adjustments needs to be done to the macro in order to eliminate roll out durations from maximum rotor speed to stand still. For Frankfurt X2 there is a visible measurement in figure 40 that probably is of this nature.

#### 5.4 Validity of the data collection

As mentioned in section 3 the data provided by STA-RMS has a resolution of one second. Data point 4 calculated the opening time of the bleed valves during roll out. Since the bleed valves shall open within one second, the macro will be unable to detect such a short duration properly. It is then not unreasonable to assume that an increased resolution, of the collected data, would be necessary in order to have proper data acquisition of data point 4.

Present in figure 30, 32 and 38 for data point 2, 3 and 5 for the Denizli dataset are visible lines created by the collected data. Having in mind the Denizli dataset is by far the largest with most start and stops it is not unreasonable to assume that this phenomena depends on a compression of data made by STA-RMS. This were examined further and the data collected have for some measurements been rounded of to the nearest integer probably in order to limit the file size.

For the Denizli dataset it can be seen in figure 29, 35 and to some degree in figure 45 that the collected data exhibits a sudden reduction in dispersion of the collected data at 17000 EOH. When the corresponding data is plotted against ambient temperature this is visible by the dataset being divided into two fields, visible in figure 28, 34 and 44. This could be indicative of changed start up settings or variations in fuel energy flow since it shows shorter durations for all the affected data points. Even though the noise from the unreasonable data is visible it also shows that the agent has the capability to pick up a change in GT operation.

Data point 7 calculates the accumulated deviation of the actual bleed valve position and the set point in order to assess if any resistance is present when operating the valve.

Data point 7 was a late addition and that is also the reason it has not been examined during the manual collection of data. This data point is different from the rest because it is not a temporal interval but an accumulation of the deviation between the bleed valve open fraction set point and the actual open fraction, also described in section 3.3. In figure 46 the open fraction and open fraction set point is plotted for two successful starts. Comparing the difference between the open fraction and their corresponding set point shows that it is visible that the graph to the right has a larger deviation. This probably depends on the compression of the data and therefore the actual open fraction set point is not conveyed properly. For standard regulation of a valve the control set point should have more "steps" and approximate the actual open fraction more similarly. For the agent this means it is dependent on a higher resolution of data in order to collect data properly. Noticeable in figure 45 for data point 7 the Denizli dataset exhibits a reduced dispersion after 17000 EOH.

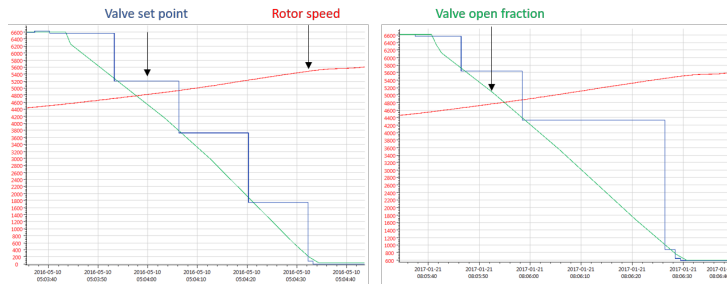


Figure 46: Two successful starts of the Denizli site shows how the difference between the set point and open fraction can vary.

## 5.5 Source of error

During the transient model valve update, the equations of the bleed and fuel valves were updated in order to provide a corrected model to be used during the simulations. The equations were produced from the manufacturer valve speci-

cations for the flow characteristic. The information were provided in a tabular form. Since the valve characteristic of the model is determined by equations an estimation had to be made from the tabulated data in order to fit an equation. When estimating an equation to fit certain data there are always some discrepancies regarding the fit. Despite this the error is limited and probably have limited consequences for the validity of the model.

The manual data collection were conducted by measuring the relevant data points manually using the RMSview software provided. In general all cases including a manual data collection of this kind include an inevitable risk for mistakes to be made during the data collection and must in this case also be taken into consideration. What should also be taken into account regarding the manual data collection is the amount of examined data, mentioned in section 4.2. Additional measurement might be needed in order to increase the certainty when making conclusions about the machine behavior. Since the data were collected at different occasions during the lifetime of the sites, this might be reason for concern regarding the ability of the collected data to convey the behavior of a machine justly.

The macros produced for the automated data collection has been discussed and it shows from the collected data that many measurements are unreasonable. The macros are not perfect and must be reviewed in order to used with the transient model.

## 6 Conclusion

The purpose of this thesis was to examine several start ups in order to provide a basis for a new type of monitoring method which includes using the transient model for comparison. This section answers the questions formulated in section 1.3.

- *Can a transient model of a gas turbine be used to predict faults in a fleet of gas turbines?*

From the manual data collection it is evident that the the model displays a similar behavior for most of the data points and has little or no variation between sites or ambient conditions. The collected data for data point 1 does not exhibit the same constant behavior as the model. This shows that the data collection can reveal faulty control valve characteristics and incorrect values of the LHV in the control system. Making data point 1 suitable for further development and implementation. For the remaining data points the model displays a constant deviation from the collected data and it can be concluded that the model is suitable for monitoring GT start ups for these data points.

- *Is the collected data suitable for the prediction of deviant behavior of a GT?*

As mentioned in section 5.3 the transient model were never used for comparison to the collected data. Despite this the automated collection of data provided information regarding the validity of the chosen data points. Data point 4 and 7 should be omitted from the automated data collection since the function of the macros used for these data point most likely is dependent on the resolution of the data provided by STA-RMS. It can be concluded that given the time to adjust the parameters of the remaining macros they can be implemented together with the transient model in order to predict deviant behavior.

- *Can a quality factor be created for the start and how should it be designed?*

Developing a quality factor related to the start demands from the collected data to be somewhat predictive. Considering the variations of data point 1 between the sites, in figure 20, it can be difficult to define an interval of where the duration of data point 1 should reside since all of the starts examined were successful. For the remaining data points the delta exhibits a predictive behavior and it can therefore be concluded that they are suitable for producing a quality factor.

Since the design of the quality factor has not been addressed in this report a design suggestion will be presented in section 7.

In regards to the literature study conducted, it can be concluded from the articles reviewed that the use of a transient model as a means to monitor the behavior of a gas turbine has not been encountered. More specifically has the

use of a transient model in conjunction with similar software as Siemens DMA not been encountered. There are however a few articles that describe the use or development of a transient model, mostly for performance calculations and not monitoring purposes.



## 7 Future work

### *Agent and macros*

For practical use of the agent produced during this project an additional effort is necessary to correct the macros delivering questionable output data.

The macro for data point 4 is to some extent limited by the resolution of the data provided by STA-RMS. However, for the remaining data points the macros could benefit from an review of their set parameters. Since all of the macros are dependent on various signals to activate the counter possibly an introduction of additional signals is necessary in order to exclude or reduce the risk of the macro counting at an incorrect occasion.

Additionally should the values were the macros start to count be adjusted in order to avoid initiating the counter due to noise from the collected data.

The omission process of data in the macro created for data point 7 should be adjusted since the calculated output exhibits extreme variations.

### *Data point intervals*

Provided the macros have been adjusted and can conduct a reliable data collection, a data collection must be made. This must be done in order to formulate intervals that can be used as reference when evaluating the health of a specific machine. A suggestion on how to do this could either be to collect data from several sites over time to produce a general interval or to collect data over time for a specific machine. For the latter case this would mean the interval would be based on the specific machine making it a tailored interval.

### *Quality factor design*

In table 7 four type of faults are listed with their corresponding fault identification number. If the intervals which dictates a fault to occur for the specific data points is specified. Then if a collected measurement is out of bounds to their specified interval a notice alarm will signal the operator and the fault is categorized. The quality factor will then be made up by the addition of the fault identification numbers, clarifying how many faults have occurred. E.g. if fault 1 and 4 occurs the quality factor will consist of:  $QF = 1000 + 1 = 1001$ .

Fault type	Fault id. number
1	1
2	10
3	100
4	1000

Table 2: Quality factor example

## References

- [1] SIT AB. Historia. ([http://www.sit-ab.se/01\\_historia.html](http://www.sit-ab.se/01_historia.html)), 2018-01-30.
- [2] Hilding Elmqvist and Sven Erik Mattsson. An introduction to the physical modeling language modelica. In *Proceedings of the 9th European Simulation Symposium, ESS*, volume 97, pages 19–23. Citeseer, 1997.
- [3] H Cohen PV Straznicky HIH Saravanamuttoo, GFC Rogers. *Gas turbine theory*. Prentice Hall imprint, 2009.
- [4] Rasmus Johnsson and Sebastian Norén. Transient model of a driven compressor, 2017. Student Paper.
- [5] Marie Kvilleng. Sgt-800 engine control specification. *Siemens Industrial Turbomachinery*, 2017.
- [6] Hughes M. Challenges for gas turbine engine components in power generation. *Procedia Structural Integrity*, 7:33 – 35, 2017. 3rd International Symposium on Fatigue Design and Material Defects, FDMD 2017.
- [7] Bhargava R. Meher-Homji CB. Condition monitoring and diagnostics aspects of gas turbine response. *Turbo Expo: Power for Land, Sea, and Air*, 11:99 – 111, 1994. Volume 4: Heat Transfer; Electric Power; Industrial and Cogeneration.
- [8] A.M.Y. Razak. In A.M.Y. Razak, editor, *Industrial Gas Turbines*. Woodhead Publishing, 2007.
- [9] Suresh Sampath, YG Li, SOT Ogaji, and Riti Singh. Fault diagnosis of a two spool turbo-fan engine using transient data: A genetic algorithm approach. In *ASME Turbo Expo 2003, collocated with the 2003 International Joint Power Generation Conference*, pages 351–359. American Society of Mechanical Engineers, 2003.
- [10] Ph.D. C.A.Hall Ph.D. S.L Dixon, B.Eng. *Fluid Mechanics and Thermodynamics of Turbomachinery*. Elsevier Inc., seventh edition edition, 2014.
- [11] Mohammadreza Tahan, Elias Tsoutsanis, Masdi Muhammad, and Z.A. Abdul Karim. Performance-based health monitoring, diagnostics and prognostics for condition-based maintenance of gas turbines: A review. *Applied Energy*, 198:122 – 144, 2017.
- [12] Inc. The MathWorks. Matlab product description. ([https://se.mathworks.com/help/matlab/learn\\_matlab/product-description.html](https://se.mathworks.com/help/matlab/learn_matlab/product-description.html)), 2018-5-2.
- [13] Michael A. Boles Yunus A. Cengel. *Thermodynamics, An Engineering Approach*. McGraw-Hill Publishing, sixth edition edition, 2007.